Exploring the use of ground penetrating radar for determining floodplain function of restored streams in the Gulf Coastal Plain, Alabama

by

Samantha Waverley Eckes

A thesis submitted to the Graduate Faculty of
Auburn University
in partial fulfillment of the
requirements for the Degree of
Master of Science

Auburn, Alabama
May 5, 2018

Keywords: geomorphology, floodplain, ground penetrating radar, restored streams, fluvial

Approved by

Dr. Stephanie L. Shepherd, Chair, Assistant Professor, Department of Geosciences
Dr. Lorraine W. Wolf, Professor, Department of Geosciences
Dr. Joey N. Shaw, Professor, Department of Crop, Soil and Environmental Sciences

Abstract

Accurately characterizing subsurface structure and function of remediated floodplains is indispensable in understanding the success of stream restoration projects. Although many of these projects are designed to address increased storm water runoff due to urbanization, long-term monitoring and assessment are often limited in scope and methodology. Common monitoring practices include geomorphic surveys, measuring stream discharge, and suspended sediment loads. These data are comprehensive for stream monitoring but they do not address floodplain function in terms of infiltration and through-flow. Developing noninvasive methods for monitoring floodplain moisture transfer and distribution will aid in current and future stream restoration endeavors. Ground penetrating radar (GPR) has been successfully used in other physiographic regions for noninvasive and continuous monitoring of (1) natural geomorphic environments including subsurface structure and landform change and (2) soil and turf management to monitor subsurface moisture content. We are testing the viability of these existing methods to expand upon the broad capabilities of GPR. Determining suitability is done in three parts using GPR to (1) find known buried objects of typical materials used in remediation at measured depths, (2) understand GPR functionality in measuring varying soil moisture content thresholds on turf plots, and (3) test methodologies at a remediated floodplain in the D'Olive Creek watershed located in Baldwin County, Alabama. We hypothesize that these methods will allow us to characterize moisture transfer from

the floodplain which is a direct function of floodplain health. The need for a methodology to monitor floodplains is widespread and with increased resolution and mobility, expanding GPR applications may help streamline remediation and monitoring practices.

Acknowledgments

Countless people and many societies, associations and committee board members helped make this research possible. First and foremost, I would like to thank Dr. Stephanie Shepherd, who without her persistent encouragement and inability to give up has made me a better researcher and scientist. A huge thank you to Dr. Lorraine Wolf for guiding me through the world of geophysics and the editing process. Thank you to Dr. Joey Shaw for opening my eyes to a discipline I knew little about but has helped in understanding my research much deeper. I owe many thanks to David Lawrence, Beth Guertal and Greg Jennings for allowing me to use their resources, equipment and research space for my project. I thank Christian Parke, my undergraduate research aide, for helping conduct field research and lug large containers from location to location. A huge thanks goes to Jeremy Menzer and participants at multiple conferences that gave me valuable feedback and knowledge towards improving my understanding of geophysics. And last but not least, I would like to thank Allen Clements for the guidance and calm patience of support.

Table of Contents

List of Figures

List of Tables

List of Abbreviations

GPR	Ground penetrating radar
USDA	United States Department of Agriculture
NRCS	Natural Resource Conservation Service
CMP	Common mid-point
CR	County road
WMP	Watershed management plan
RBD	Relative dielectric permittivity
EM	Electromagnetic
TDR	Time domain reflectometer

INTRODUCTION

The need for broad, easy-to-use monitoring practices within remediated or restored stream sites is more necessary than ever. More than 15 billion dollars has been accounted for annually in domestic, ecological restoration through indirect economic impacts of restoration activities in the United States, and at least 18% of ecological restoration is focused on aquatic and riparian restoration and management (BenDor et al., 2015). Stream restoration projects are expected to expand in the future, particularly in urban areas, and the need for effective monitoring practices is in demand (Bernhardt and Palmer, 2007). Two critical factors to consider for comprehensive monitoring are spatial and temporal continuity. Most of the current monitoring practices focus on point data within a stream or along the stream bank (e.g., sediment load, discharge, repeat cross-sectional surveys), which lack the ability to capture the spatial and temporal complexity of floodplain, riparian, and stream processes (Johnson et al., 1995). Urban areas have expanded rapidly along coastal areas, resulting in dramatic increases in sediment loading, degradation of water quality in streams and loss of biological habitat in Alabama's coastal areas (Cook et al., 2014). Studies indicate that an increase in urbanization over the last three decades has affected low-lying coastal communities the most (Ellis et al., 2010). With this increase in urbanization, it is assumed that the need for ecological restoration and river remediation will also increase across coastal areas. Furthermore, there is rarely long-term monitoring of restoration sites to determine if the restoration was sustainable.

This research will investigate the application of ground penetrating radar (GPR) techniques to study floodplain processes after stream restoration. Since GPR is a non-invasive geophysical method, it has the potential to be a long-term monitoring practice that is easily

deployable by trained staff. Not only would a non-invasive monitoring method help communities and restoration professionals fulfill monitoring obligations, it would also help create a database of research that can be referenced over long time scales to reevaluate remediation practices. This project investigates the possibility of applying ground penetrating radar to a remediation site in a coastal plain setting as a long-term monitoring practice. Better understanding of the shallow subsurface in remediated floodplains can aid in evaluating the sustainability of these projects over longer periods.

Research Questions

GPR is a versatile methodology, currently utilized in a range of applications across multiple disciples. We hypothesize that GPR is suitable for characterizing floodplain moisture retention after precipitation events as well as documenting subsurface structure in built floodplains. To test these hypotheses we designed a three part experiment to (1) find known buried objects of typical materials used in remediation at measured depths, (2) understand GPR functionality in varying soil moisture content thresholds on turf plots, and (3) capture moisture content within remediated floodplains in a case study in the D'Olive Creek watershed located in Baldwin County, Alabama. The goal of this research is to use known applications and post-processing techniques to study critical processes of moisture retention in floodplains because this reduces runoff and erosion, a common goal in urban stream restoration.

BACKGROUND

The D'Olive Creek watershed lies on the western edge of Baldwin County (Figure 1) and encompasses approximately 7,700 acres and 23 miles of streams (Coffee, 2010). The change in land-use patterns throughout the county has contributed to the impairment of the main tributaries in the watershed, which flows directly into Mobile Bay estuary, negatively impacting estuary health (Vittor, 2010). Over the last three decades, the cities of Daphne, Fairhope, Gulf Shores, Foley, Robertsdale and Spanish Fort have experienced significant urban growth (Ellis et al., 2010). Maintaining water quality and estuarine resources in the Mobile Bay has been of concern since the mid 90's because rapid urbanization led to increases in storm-water runoff and pressure on infrastructure (Lambin et al., 2001; Cook, 2008; Cook et al., 2014). This pressure on infrastructure has manifested as stream and floodplain erosion, loss of riparian density, and habitats, and has affected Daphne and Spanish Fort as two of the fastest growing areas in Alabama. In addition to urban pressures the area is also susceptible to storm surge and wind and water damage from hurricanes (Ellis et al., 2010).

The City of Daphne has responded to stream degradation by launching multiple remediation and restoration projects in the D'Olive Creek watershed designed to combat increased erosion. In 2010, Thompson Engineering completed a watershed management plan (WMP) for the three major watersheds in Baldwin County. The report suggests that an excessive amount of erosion and sedimentation have been a known problem in the D'Olive Creek watershed since the 1970's (Coffee, 2010). The WMP specifically acknowledges that urbanization in the area has exacerbated concerns of erosion because it was previously forested, which kept rain splash and other erosive mechanisms at a minimum.

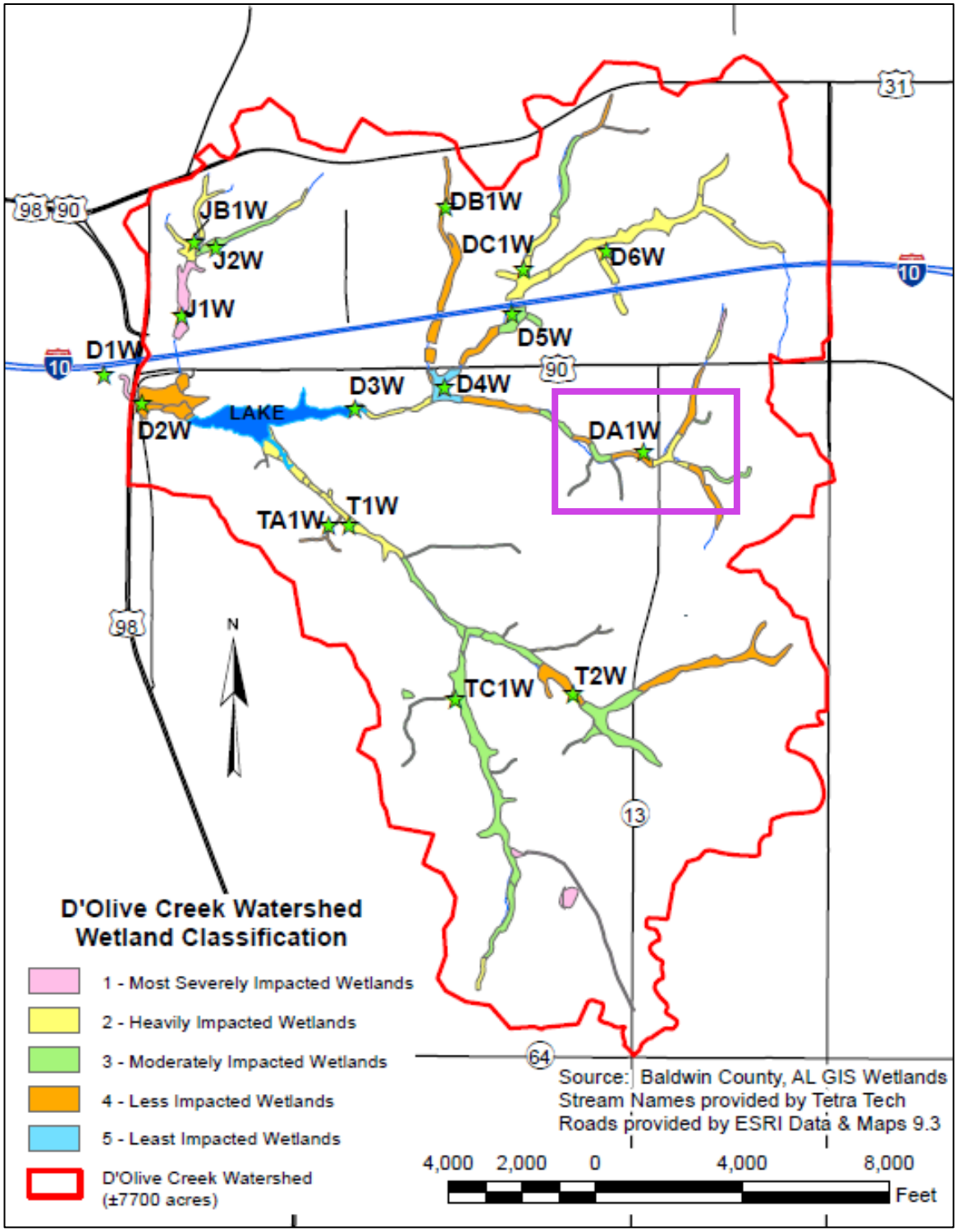

Figure 1. Map of the D'Olive Creek watershed compiled by Vittor (2010) depicting the most impacted wetland areas within the watershed. Purple box indicates D'Olive Creek study site.

Surfaces such as asphalt, concrete, and compacted soils from development prevent the recharge of water into the subsurface and increase the risk of erosion at the surface (Ellis et al., 2010). At the time of the WMP, the D'Olive Creek watershed ranged from 20-25% of impervious cover, with a potential for increase to 38% by 2020 (Coffee, 2010).

Watershed stakeholders working with restoration professionals and researchers at Auburn identified critical research questions pertaining to the D'Olive Creek watershed in order to improve ongoing restoration and management efforts (Brantley and Knappenberger, 2016). These questions have guided the focus and scope of this research. Specifically, stakeholders expressed a need to validate proposed and existing channel restoration design by utilizing different survey technologies (in this case GPR), as well as understand how restoration efforts alter the balance of ground and surface water.

A primary goal of stream restoration in the D'Olive watershed is to address issues by stabilizing floodplains with vegetation and increasing infiltration within the floodplain, which decreases erosive runoff (Violin et al., 2011). Current monitoring practices in the watershed are focused on point-source data, such as sediment load measurements and repeat geomorphic surveys (e.g., Cook, 2008; Cook et al., 2012; McMillian and Noe, 2017), but these methods do not have spatial continuity and cannot assess floodplain function. In order to have successful, long-lasting restoration, we should develop methods to quantify and monitor floodplain function. Healthy floodplain functions including floodplain connectivity, water quality, channel morphology, channel structures and the native plant community are integral to the long-term sustainability of stream and floodplain re-evolution. These characteristics ultimately contribute to the ability of the landscape to intake moisture and transfer it to stream channels.

Increasing floodplain function and connectivity in urban watersheds is challenging due to imperviousness and storm water conveyance systems that can undermine completed restoration projects (McMillian and Noe, 2017). Choosing the most effective functional restoration characteristics (e.g., floodplain connection versus channel structures) while also considering space restrictions can be difficult.

Regional Geomorphology and Geology

The geomorphology in the upper part of the Mobile Bay is dominantly controlled by conventional stream dynamics and is the remnants of the drowned portion of an incised valley and its alluvial plain, draining south to meet the Gulf coastline (Smith, 1988). Estuaries like Mobile Bay and others along the Gulf Coast have been filled with sediment from fluvial and marine sources. Estuarine deltaic deposits in the area are a result of the rise and fall of sea level along the continental shelf over the last 10,000 years (Davis, 2010). Elevation change within the D'Olive Creek watershed is higher than other adjacent watersheds (Salisbury, 2018). It is believed that the unique nature of the high topography in the D'Olive Creek watershed is due to a historic natural sediment load greater than other small coastal watersheds. This has created much of the sediment accretion as well as sediment erosion and removal to the Mobile Bay (Coffee, 2010).

The underlying stratigraphy effecting much of the sediment accretion and erosion to the coast consists of Tertiary and Quaternary-aged sediments (Figure 2). Tertiary sediments consist of sand, silt, gravel, clay, and sandstone. Miocene (Tmu) and Pliocene (Tci) are undifferentiated sediments dominated by clay, sand, and sandy clay. Some dolomitic fossiliferous limestone is

expressed down-dip of the lower part of the series (Reed, 1971). The Quaternary System, containing the Pleistocene Series (Qt), overlies older units in the form of large terrace deposits that are adjacent to the Mobile River. The terraces are mostly composed of coarse-grained sand with lenticular beds of sandy clay at some localities (Reed, 1971). Above the Pleistocene Series lies alluvial deposits that are from both Pleistocene and Holocene Series (Qal). The alluvial deposits consist of deltaic, alluvium, beach and terrace deposits (Reed, 1971).

Overall, the deposits in this area are no thicker than 150 feet and are mostly unconsolidated or weakly cemented. The D'Olive Creek watershed is dominated by the presence of the Citronelle Formation (Tci) and the Miocene Series undifferentiated, which consist of gravelly sand with a thick layer of clay 25 feet below the contact (Reed, 1971). It is important to note the study site has since been remediated thus some floodplain sediments are anthropogenic in nature, no longer representing the original stratigraphy.

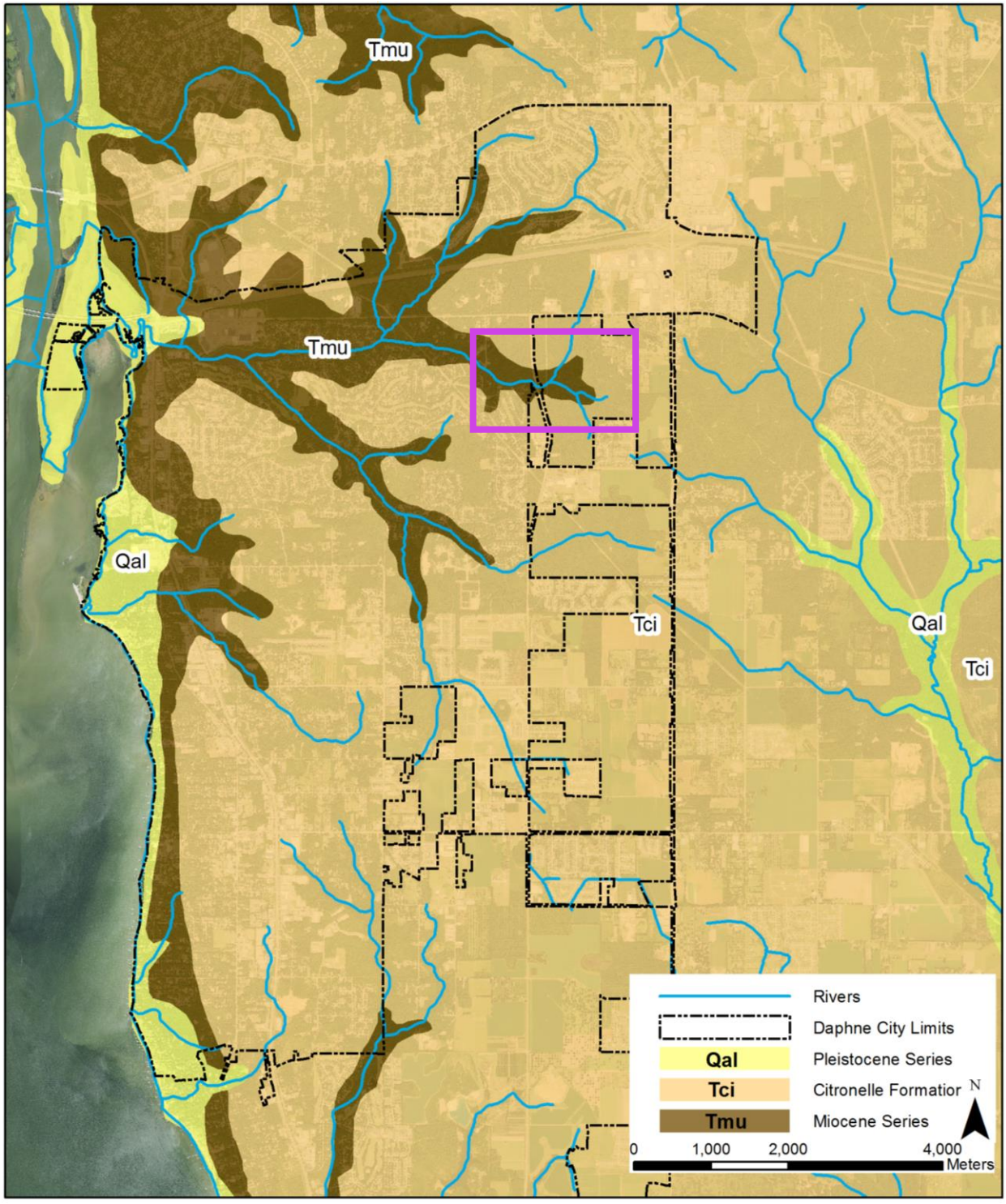

Figure 2. Geologic map adapted from Special Map 94 (Reed 1971), showing outcropping units within Baldwin County. Purple box indicates study site.

D'Olive Creek Study Site

The study site (Figure 3), located off CR 13, just south of I-10 in Daphne, Alabama includes reference, restored/remediated, and disturbed reaches. The study area lies among the middle and upper tributaries of the D'Olive Creek and encompasses approximately 1,161 acres (Coffee, 2010). Groundwater sourcing the watershed comes from the Miocene-Pliocene aquifer, consisting of the Citronelle Formation and undifferentiated deposits (Coffee, 2010).

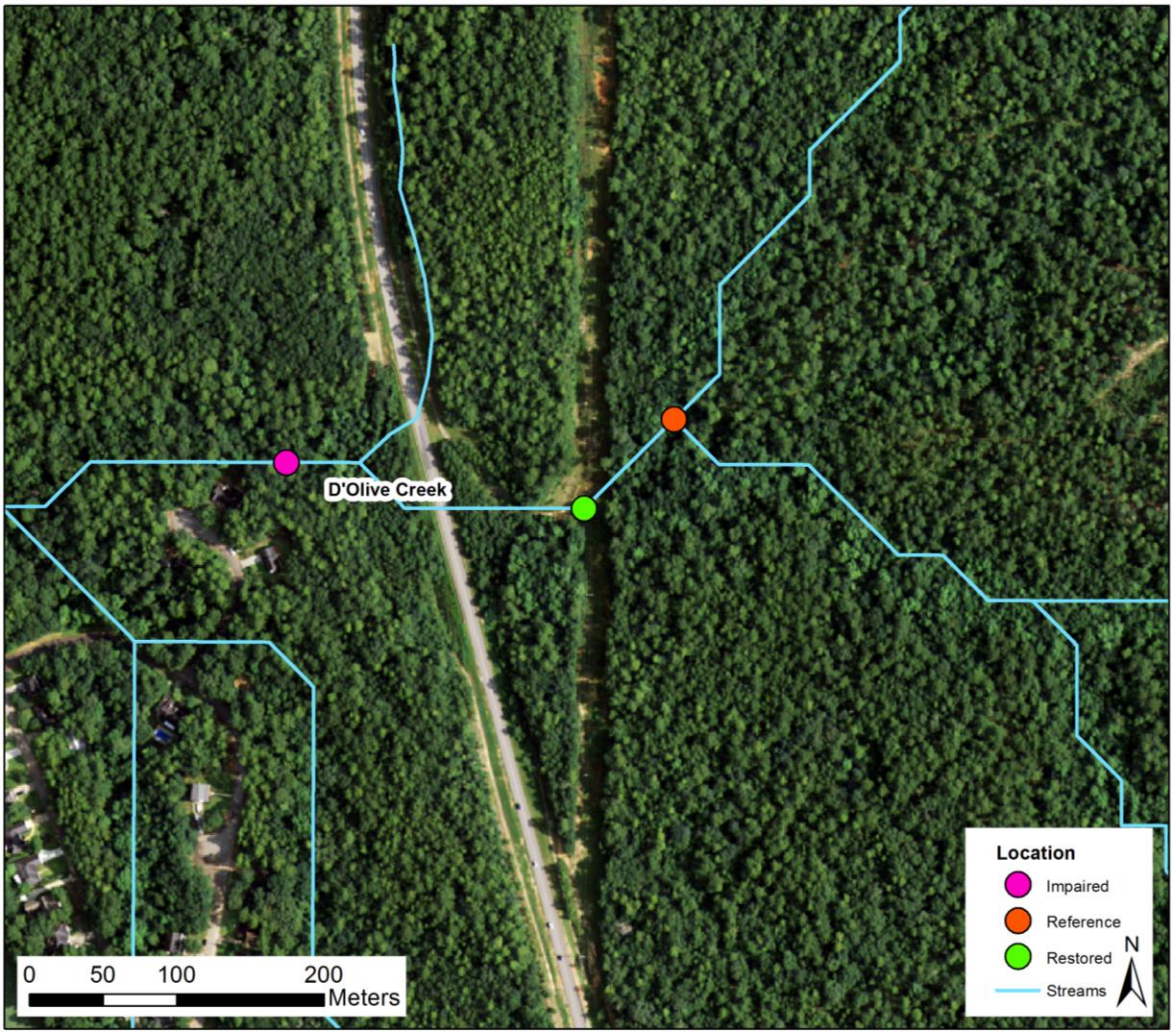

Figure 3. Aerial image map of D'Olive Creek study site. Green circle indicates area of restored site where GPR data was taken.

Stream degradation and the subsequent restoration process completed last year at this site has been well documented by the City of Daphne. Current geomorphic conditions, riparian health, and possible drivers of impairment are being studied using GIS analysis and traditional stream surveying techniques at three reaches: a reference reach, a restored reach and an impaired reach (Salisbury, 2018). The impaired reach of D'Olive Creek, on the west side of CR 13, is highly entrenched, down-cutting through hardened clay layers (Figure 4). It flows from a large culvert under CR 13 and receives water inputs from paved run-off channels adjacent to the highway (Coffee, 2010). Both the restored and reference reaches are east of CR 13. The reach of the stream is terminated on both west and east sides by housing developments and urbanized areas. Overall, this site is indicative of the incision observed throughout the watershed and the current restoration approaches being undertaken locally. Additionally, the restored site is relatively open, i.e., low-lying vegetation and few trees, making it suitable for acquisition of GPR data surveys.

Figure 4. Images taken at the D'Olive Creek impaired site where the creek has incised through a resistant clay layer and is no longer able to access its floodplain.

Ground Penetrating Radar

GPR is a geophysical method with broad capabilities that could be applied to long-term monitoring of floodplain function. GPR is nondestructive and has been widely used to image surface and subsurface geologic features, such as dunes or bedding planes as well as soil moisture in agricultural settings to implement accurate irrigation practices and monitor freshwater/saltwater interactions (Hubbard et al., 2003; Van Dam et al., 2003; Jol, 2009). Other common applications of GPR technology include construction, demolition and highway infrastructure (Grote et al., 2002). Research conducted on measuring volumetric and gravimetric water content as well as soil water distribution with GPR has been initially established and has set the basis for the methodologies conducted in this study (Steelman and Endres, 2012).

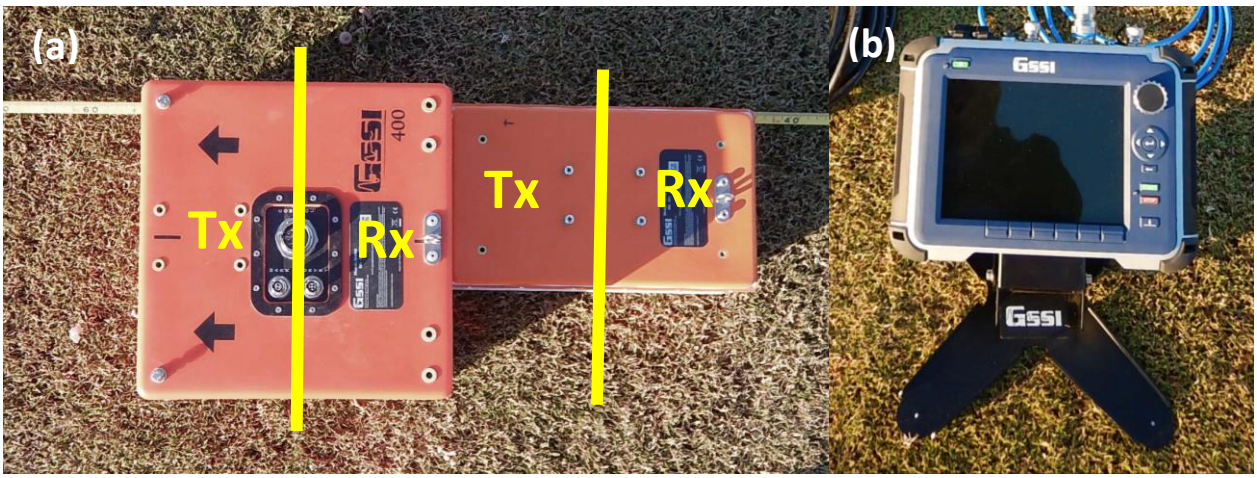

Figure 5. (a) GSSI GPR unit including 400 MHz antenna (left) and 900 MHz antenna (right), set up to take data in a common mid-point configuration, (b) GSSI SIR 4000 control unit.

The basic components of a GPR unit consists of an antenna, a console and an encoder (GSSI, 2015). The GPR system used in this research included antennas with set frequencies (Hz), a transmitter (Tx) and a receiver (Rx). Both the Tx and Rx are housed within one plastic container that connects to a console (Figure 5). The encoder, also known as the survey wheel, controls for locational accuracy during GPR data acquisition (Bigman, 2018). When the antenna is pulled over the surface, the transmitter produces the electromagnetic signal while the receiver records responses for a defined amount of time (Bigman, 2018).

The electromagnetic pulse propagates through material and when it encounters an object, the signal is returned (Figure 6). The reflection waveform is then digitized and recorded to produce a radar profile. The strength of a reflection is dependent on the material of the buried mediums and on the environment (i.e., sediments) under investigation (Carrick, 2017).

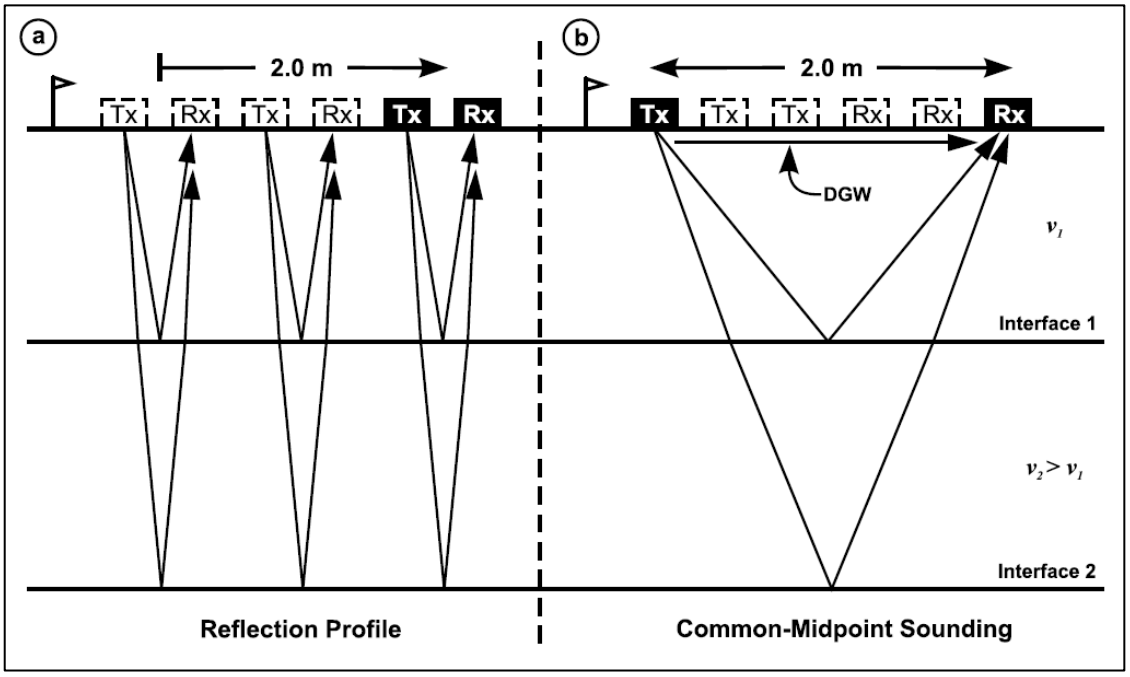

Figure 6. Two generalized GPR surveys: (a) reflection profile with one antenna and (b) common midpoint reflection profile using two antennas (Steelman et al., 2012).

The success of ground penetrating radar in geologic research can be attributed to a large contrast in relative dielectric permittivity (RDP) of target materials. Ground penetrating radar has been successfully used to study stratigraphic structures, such as lacustrine succession (Havholm et al., 2003), estuarine shorelines (O'Neal and Dunn, 2003), /dune reactivation (Botha et al., 2003) and sedimentary structures in the vadose zone (Van Dam et al., 2003). These studies were successful due to visible reflections off boundaries between layers with different dielectric constants. Changes in lithology, water content or grain size are detectable by GPR when the characteristics are different from the surrounding material or objects in the subsurface (Carrick, 2017).

Jol et al. (1995) determined that in ideal conditions, GPR can "image 'high-resolution' stratigraphy in shallow subsurface sand, gravel, and peat with the best results obtained in clean (free of silt and clay), quartzose-rich, thick, clastic sediments". Soils in floodplains and coastal environments in the study area will not be free of clay or silt, but will most likely be dominated by loamy textured sands with siliceous or kaolinitic mineralogies (USDA NRCS, 2017). While these sediments may not be ideal, GPR is becoming commonly used in all environments and in many different applications because of its ability to be site specific (Bigman, 2018). Defining areas for GPR surveys within the coastal plain can also be identified by using online databases (e.g., Web Soil Survey) and confirmed by identifying the soil profile from a local pedon.

Previous work using GPR to assess moisture content (e.g., Merz and Plate, 1997; Overmeeren et al., 1997; Grote et al., 2003; Huisman et al., 2003; Lunt et al., 2005; Grote, 2013; Forte and Pipan, 2017) suggests that this technology holds promise for long-term monitoring of floodplain function. Assessing moisture content in the subsurface is done using a common

multi-offset mode, also called common midpoint reflection (CMP). Two antennas of different frequencies run in tandem to produce an image (Figure 6b). Direct ground waves acquired during a CMP sounding can determine changes in vertical shallow subsurface moisture content, allowing us to model moisture content in floodplains (Steelman et al., 2012). Estimated water content is determined to be increasing or decreasing based on velocities calculated from the post-processing software (Jol, 2009). We hypothesize that velocity estimated from each GPR survey will increase as moisture content in sediment decreases.

Most GPR applications utilize single-offset measurements rather than CMP measurements, but single-offset measurements cannot be used to determine water content of soil layers if there is no information about the known depth of a placed reflector (Huisman et al., 2003). Although the scholarly literature states CMP surveys are an effective method to estimate soil water content, it is highly dependent on material and antenna frequency (Overmeeren et al., 1997; Grote et al., 2003; Huisman et al., 2003; Lunt et al., 2005).

Measuring moisture content from GPR data is done by calculating ground wave velocity of soil with two layers of contrasting dielectric permittivity or measuring ground wave velocity over time. Since the GPR waveform change is dependent upon the attenuation of electromagnetic radiation in the medium and its reflection from the soil boundary, moisture content can be calculated in the same place over time (Khakiev et al., 2014).

Allred et al., 2016 and Freeland et al., 2016 have both successfully used CMP methodology to map moisture in sand layers on golf course putting green. They compared GPR to time domain reflectometry (TDR) and found that TDR was only able to measure the volumetric water content near the surface and not far enough into the subsurface. The success

found in these two studies was that GPR was able to measure an averaged volumetric water content over the entire thickness of the sand layer.

A similar study was conducted at Robert Mondavi Winery in California by Grote et al., (2003). This study determined that GPR surveys were proficient at noninvasively estimating shallow water content in a rapid timeframe. Grote et al., (2013) calculated ground wave velocity by identifying the difference between the air wave and ground waves. Using calibration equations adapted from Huisman et al., (2001), they were able to convert their GPR CMP data to an estimated volumetric water content. It is important to note that most of the studies using GPR actively avoid soil materials with heavy clays due to attenuation problems. Due to the nature of coastal plain sediments in Alabama, avoiding clay-rich material is unavoidable.

Overmeeren et al., (1997) also successfully used GPR CMP measurements to estimate moisture content of the subsurface. This study identified clear interfaces between layers with different propagation velocities. This type of CMP velocity analysis may pose a problem in remediated floodplains, where subsurface interfaces may not exist due to human disturbance; however, if a ground wave can be identified, moisture content can be estimated.

Determining if the proposed methodologies will be successful in capturing moisture content of restored floodplains is dependent on multiple experiments, all with different objectives. The buried objects experiment is hypothesized to produce returns of buried materials in coastal plains sediments. The turfgrass moisture plot experiment is expected to narrow down functionality potential of GPR in varying soil moisture content thresholds. These two experiments are then applied to a case study site to capture moisture content within a restored floodplain in the D'Olive Creek watershed.

METHODOLOGY

In order to address the objectives of this project, three experiments were conducted to test the validity of applying GPR methods to study restored, i.e., built floodplains. The first experiment involved burying known objects in a trench in order to calibrate the GPR techniques to coastal plain sediments with high levels of clay that could attenuate the radar signal. This experiment was done at EV Smith Research Center in natural soils that represent floodplains parent material with agricultural land use (Figure 7). The second experiment focused on documenting moisture changes through time in an engineered soil at the Auburn University Turfgrass Plot, where irrigation coverage allowed for maximum ground saturation. The third and final experiment allowed us to apply the methods tested in the first two experiments to a remediated floodplain in the D'Olive Creek watershed (Figure 1).

Auburn University Extension Research Centers

The Auburn University Turfgrass Research Unit and the EV Smith Research Center are two research properties owned and operated by the College (Figure 7). The EV Smith Research Center is located in Shorter, Alabama, off CR 40 in Macon County, and is mainly used for agriculture research. The plot used for this project was planted prior to surveys being conducted, but it had no active crop growth at the time of data acquisition. The AU Turfgrass Research and Education Center is a part of Auburn's main campus and is located off Shug Jordan Parkway in Lee County, Alabama.

These two sites were chosen for large, cleared areas, allowing enough space to set up GPR survey grids. The soil profiles between the two sites differ in composition and soil type,

allowing the GPR to be utilized in varying coastal plain deposits. The two sites are approximately 35 miles apart, but span two counties and very different soil profiles (e.g., composition, clay content and grain size).

Figure 7. Map showing locations of the EV Smith Research Center (red star) and the Turfgrass Research Center (blue star).

Experiment I: Buried Objects

The viability of locating and identifying buried objects for floodplain management was completed at the E.V. Smith Research Center. Determining the trench location was done through the Web Soil Survey database using a GPR suitability function based on soil series and clay content (Figure 8). A 2-meter-deep trench was dug using a backhoe and a soil profile was recorded from the north wall of the trench. Field characterization of the soil helps determine the amount of attenuation a radar signal would exhibit, improving results.

Figure 8. Soil map generated by Web Soil Survey (USDA NRCS, 2017) showing suitability of GPR for different soil types based on texture, composition and slope.

Common objects (logs, rebar, rock, etc.) found at remediation sites were buried at two depths within the trench. Also two large plastic containers were buried to simulate a detectable void space in GPR reflections. The first set of objects placed in the bottom of the trench includes a blue and white plastic cooler, two wood logs, an irregular cement block and a boulder sized piece of salmon colored quartzite (Figure 9 and 10). A section of rebar was hammered into the west wall at 1.9 m. The depth to the top of each item was measured and recorded. Objects were covered to a depth of 1 meter, and the second set of objects were placed on the sediment fill. This set included two sections of rebar placed on the covered surface, one piece of rebar hammered into the west wall, a second irregular cement block, one boulder-sized piece of limestone, a 6-liter blue plastic carboy, and four wood logs. The depth to

the top of each object was again measured and recorded. The trench was the filled with a backhoe. After the trench was filled, we let it settle for 5 days before returning the take GPR data.

After settling, the top of the trench was concave in shape so more soil from the original excavation was put on top of the trench with shovels and smoothed out to allow for even GPR data acquisition. GPR data were then taken in perpendicular transects (forming a grid) over the filled trench to determine if any or all objects could be detected within the subsurface. Both the 400 MHz and 900 MHz antennas were employed to determine the depth of buried wood logs, boulders, rebar and void spaces created using plastic cooler/carboy (Figure 10). The data taken at EV Smith were then transferred from the console to a dedicated GPR field computer. The data were processed using RADAN 7™™, the software produced by GSSI, to produce a subsurface image.

Figure 9. Images of the specific objects buried at EV Smith Research Center including: (a) six logs, (b) four of six pieces of rebar, (c) two rocks and two blocks of cement, (d) a rectangular cooler, and (e) a 6 liter carboy.

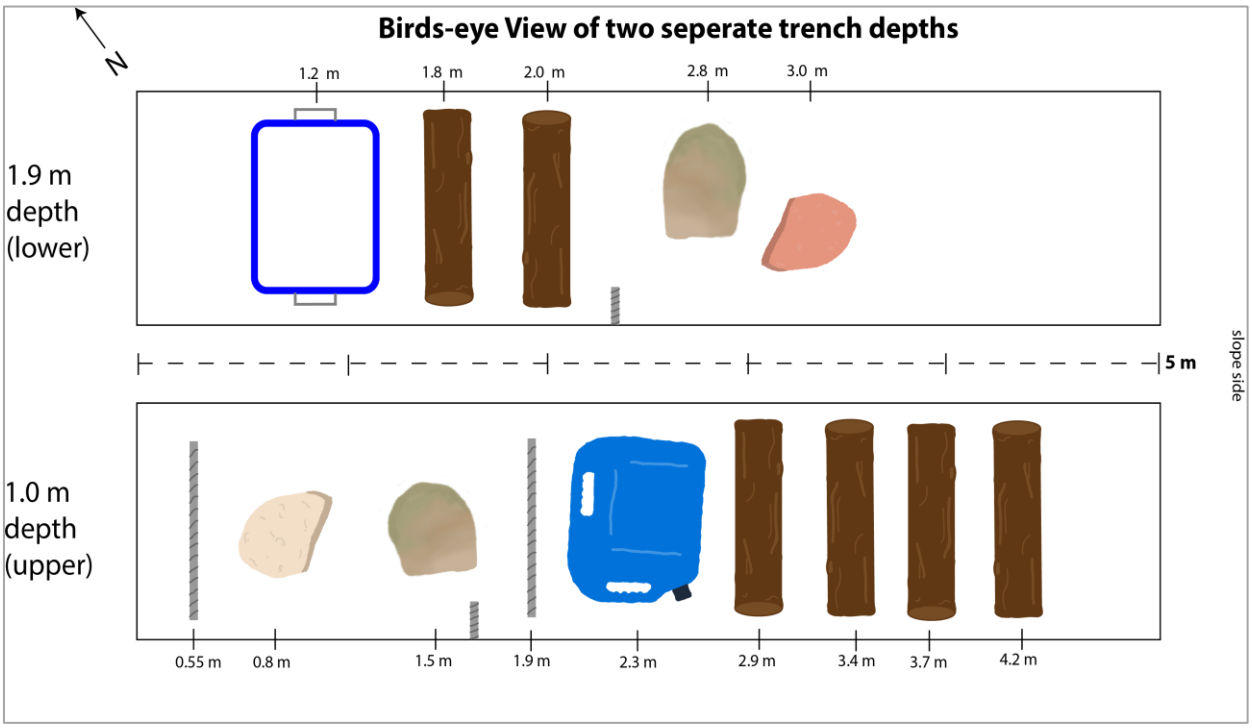

Figure 10. Illustration depicting objects buried at EV Smith Research Center in a 7 m x 1 m trench at two depths (approx. 1 m and 1.9 m).

Experiment II: Turfgrass Plot Moisture

A 10 m x 10 m grid was set up on a southwest plot on the Auburn University Turf Research Unit. The plot was saturated from the surface to a depth of approximately 2 m using overhead sprinklers with rotor heads that have head to head coverage, ensuring even watering (D. Lawrence, personal communication, October 10th, 2017). CMP data were taken every other day for two weeks to capture a full cycle of drying from saturation (Figure 11). Step increments for CMP data included an initial offset of 32 cm and 0.5 m after the first point was taken (Figures 5 and 6). Continuous GPR data were taken in perpendicular transects with 0.5 m increments and later combined to create a 3D profile of the subsurface. The latter set of data was taken to supplement the CMP data and to determine if any soil horizons could be detected.

Figure 11. Image of GPR data acquisition on turf plot. Purple box indicates area of 10 m x 10 m grid and orange flags are markers for 1 m spacing.

The GPR antennas used in the survey included both 400 MHz and 900 MHz and both were used to run profile grids as well as CMP profiles. CMP profiles were orientated in a cross shape: one in an east-west orientation and one in a north-south orientation (Figure 12). The center coincided with the 6 m mark on both sides of the grid and crossed in the center. This orientation was used because it utilized the maximum area of the plot and touched all four sides, allowing for moisture measurements to be evenly distributed across the study area. GPS points were also taken where blue Xs are marked on the plot using a Trimble Geo 7X.

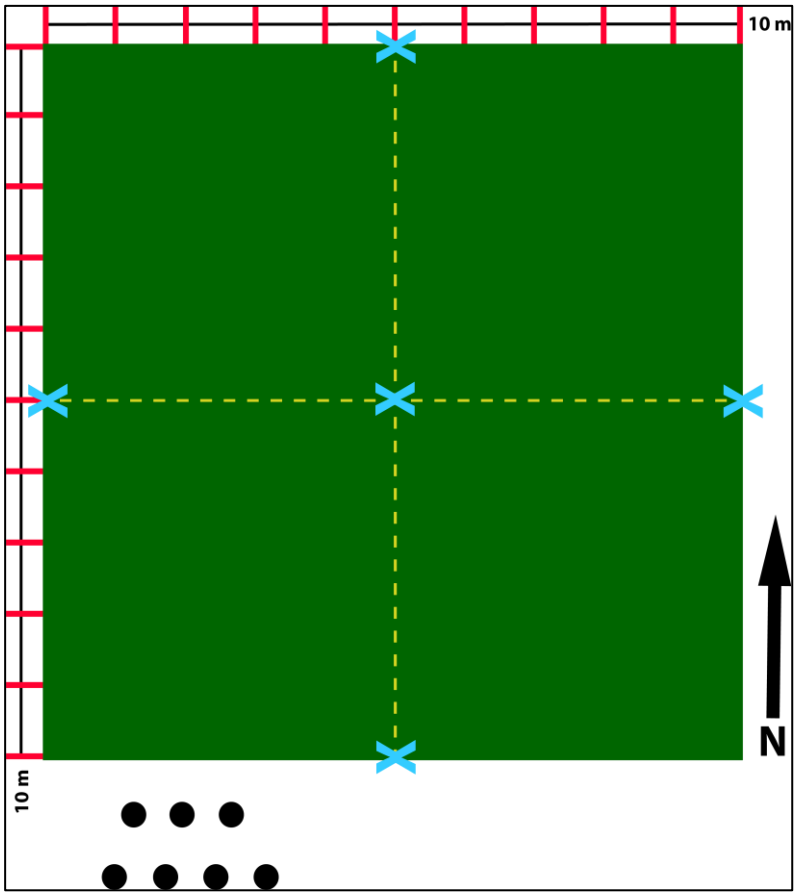

Figure 12. Diagram depicting set up for GPR survey on turf plot. Red lines indicate spacing for 2D GPR passes, blue X's are POGO survey locations, yellow dotted line is CMP survey passes, and black dots are soil auger sample locations. CMP passes are line 1=E-W pass, line 2=N-S pass.

Soil auger measurements were taken concurrently with GPR data to capture volumetric water content by percent. Auger samples were taken at two depths, approximately 0-7 cm and 55-65 cm, to get gravimetric water content of the subsurface. Gravimetric water content was then converted to volumetric water content by percent with the following equations (when the mass and volume of water are equal):

$$m_{water} = m_{wet} - m_{dry} \qquad \theta_g = \frac{m_{water}}{m_{dry}} \qquad \theta_v = \frac{volume_{water}}{volume_{soil}}$$

In order to get gravimetric water content, a consistent sample size must be obtained. This was done using a sampling head with removable sample tubes that was attached to the hand auger (Bilskie, 2001). One sample was collected from each depth (~7 cm and 55 cm), for a total of two samples every other day. The samples were weighed, then dried for 48 hours at 115 ˚C, then weighed again. The difference in mass was used to calculate volumetric water content (Bilskie, 2001).

We also employed a POGO meter to confirm the measurements taken with the hand auger (Figure 12). The POGO meter takes direct volumetric water content measurements, and was used at five evenly spaced locations on the grid. We compared the water content derived and calculated from auger samples to the direct volumetric measurements from the POGO meter.

Experiment III: D'Olive Creek Case Study

Once the control experiments were completed at the Turfgrass Research Unit and the E.V. Smith Research Center, the methodologies were applied at the case study site in the D'Olive Creek watershed in Daphne, Alabama. A 10 m x 10 m plot was set up on the northern floodplain of the remediated stream reach of D'Olive Creek (refered to as CR 13 Site). The GPR was used to take 2D profiles as well as CMP data. The 2D profiles were taken to see if remediation structures built into floodplains could be identified in the subsurface. These data could be used later to create an 3D subsurface image by combining perpendicular 2D profiles. CMP data was taken to determine moisture content of the floodplains, and to assess how well moisture is being secured and retained in the subsurface in remediated conditions. To calibrate the moisture data from the GPR CMP survey, an auger hole was used to obtain gravimetric water content. POGO meter measurements were also taken in three sections of the 10 m x 10 m plot. These data was later post processed and analyzed for accuracy.

Ground Penetrating Radar Post-processing

Two geophysical software programs were used to post process the GPR data taken in all experiments (Figure 13). RADAN 7™™ (RAdar Data ANalyzer) was created by GSSI to be compatible with their GPR equipment and can only process files recorded by GSSI equipment, while ReflexW™™ was used to process a multitude of different geophysical data files.

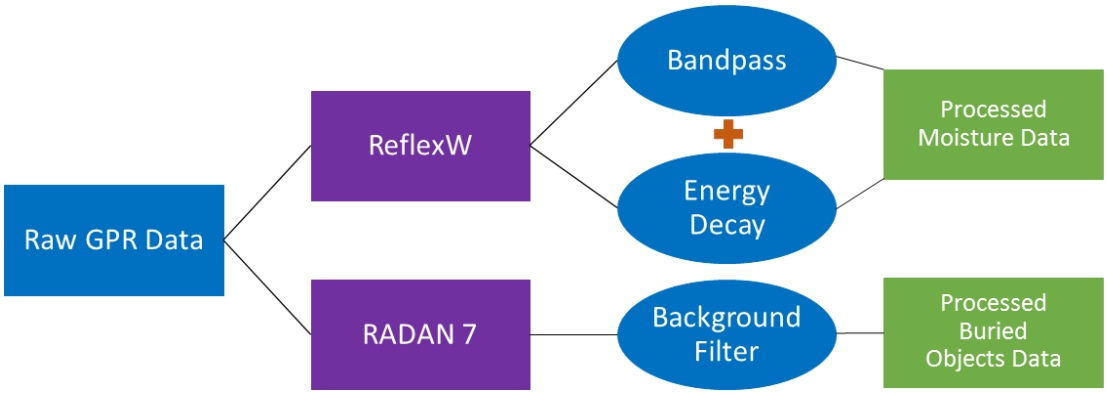

Figure 13. Flow chart describing two types post-processing applied to raw GPR radar. Rectangles represent data products and ovals represent data processes.

RADAN 7™ Processing

RADAN 7™ was primarily used for processing 2D profiles and creating 3D representations from the buried objects experiment. Each file was processed through a series of steps to correct for noise to be easier to interpret. The first step in RADAN 7™ is to correct for the transition of the waveform from the air to the ground via the antenna. This is known as adjusting to time-zero and is built in function in RADAN (Carrick, 2017). This process is important because it causes depths of targets to be exaggerated if the signal is not adjusted. Display gain was usually adjusted in greyscale to enhance reflections. Display gain does not change the data within the file; instead it enhances visual contrast in order to detect hyperbolas more easily. Hyperbolas are radar reflections seen in a radar profile and indicate a change in velocity of the propagating waveform. The general background removal filter was applied to remove ringing and to correct for consistent horizontal noise. Background removal was necessary in some of the profiles to eliminate horizontal banding not correlated to existing lithologic boundaries (Carrick, 2017). Migration was not applied to the buried objects profiles

because it increased the difficulty in determining locations of reflectors by collapsing the hyperbolas. No bandpass filters were applied since there was very little or no large scale ringing, which are small reflections that create random noise in the data. Depths of objects seen in 2D profiles were determined by the x axis and the cursor to define the exact depth in meters.

ReflexW™ Processing

Since RADAN 7™ has limited capabilities for processing CMP data, ReflexW™ was used to process CMP data taken at during the Turfgrass experiment and at the D'Olive Creek site. ReflexW™ was chosen for its ability to accept any GPR file type and for its broad spectrum of processing capabilities.

The "2D-dataanalysis" processing function in the ReflexW™ software was used to process the initial CMP data was. Files were imported and given specific import coordinates and plot options (Figure 14). Once import was complete, a band-pass filter was applied to the data. This was done using a Butterworth filter with a lower cutoff of 200 MHz and an upper cutoff of 600 MHz. The decreased data noise that appeared as thick black lines in the profile. The next step was to apply an energy-decay filter, which is a type of gain filter. The energy-decay was applied to all traces and had a scaling value of 1. A time-zero correction was tested but it was found to be unnecessary after both the band-pass and energy-decay filters were applied. Since the original offset of 0.32 m is close to zero, there was no visible difference to the data when a time-zero filter was used.

A velocity inversion was applied to all identifiable direct reflections in each post processed profile using the interactive velocity analysis within “2D-dataanalysis” in ReflexW™. The first arrival of the ground wave is identified and the slope can be used to calculate velocity. Based on the behavior of EM waves, we will infer moisture content based on velocity changes. Due to difficulty in making picks to calculate velocity (selections of peaks representing energy returns), this method was abandoned as a reliable method for inferring moisture content.

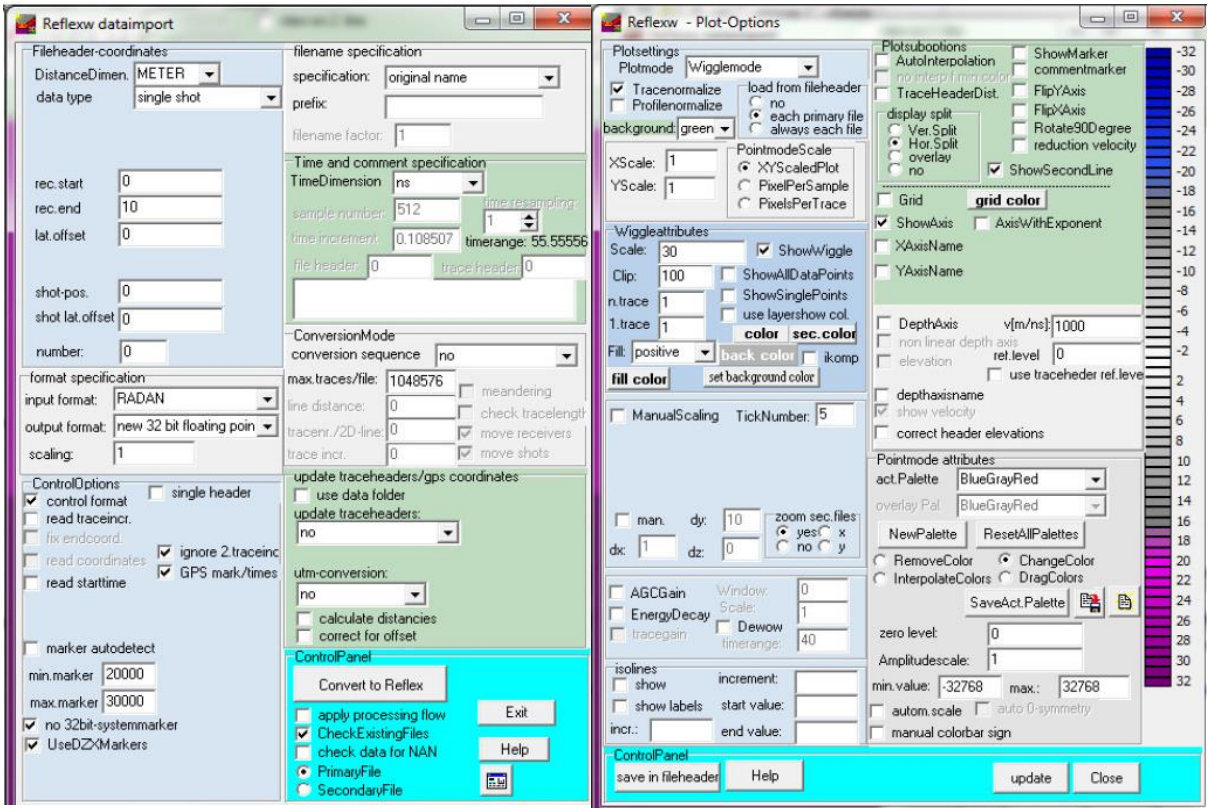

Figure 14. Data import box (left) indicating the correct parameters for file import in ReflexW™. Data plot options box (right) indicating settings for reflection plots.

Instead, three averaged arrivals from each profile were used to calculate reflector depth using a two-way travel time that was estimated from the first clear reflection and measured

from the x-axis on each processed profile. With the assumption that the first clear reflector in the same profile line is fixed, the velocity determined from this function will then be used in the following equation to infer if velocity (and hence moisture content) is changing over time:

$$t = \frac{x}{v}$$

In the equation above, t= two-way travel time, x= distance travelled by wave, and v= velocity (ns/m). We adapted the methodology of Huisman et al., (2001) to make broad assumptions about subsurface moisture content based on velocity trends within a profile. We are expecting the velocity to increase with time as the subsurface dries.

RESULTS AND DISCUSSION

The three experiments validate the potential of utilizing GPR methodologies to estimate moisture retention in build floodplains with limitations associated with both the instrumentation and the floodplains sediments. While each experiment had its limitations, the combination of all three studies shows promise for the continued testing of these methodologies.

Although three types of surveys – 2D with 400 MHz antenna, 2D with 900 MHz antenna and CMP – were completed at all study sites, a larger part of the data was found to be unusable (Table 1). While not all these data were used in the final analysis, it was vital to test different GPR configurations in order to determine the optimal set up for each site and experiment objectives. This resulted in many GPR surveys that were unusable had inconsistent field conditions, or lacked usable returns. The 2D surveys taken at the Turfgrass plot yielded no moisture data and therefore are not included in the results. Also, data from the CMP survey taken at the buried objects sites, did not reveal any subsurface moisture trends due to clay content and high attenuation. The surveys marked with a “U” in Table 1, were processed and used in the final GPR analysis. The data labeled “A” did not produce viable data for the experiment objective.

Table 1. Summary of all GPR survey data taken at three experimental sites involved study. (BO= buried objects site (EV Smith), MO=moisture plot, DO=D'Olive study site. ** denotes incomplete survey during time of acquisition)

Date	Site	Type of Survey	Antenna	# of lines	N-S	W-E	Used/ Abandoned
10/1/2017	BO	2D	400	47	15	32	U
10/1/2017	BO	2D**	900	11	11	0	A
10/1/2017	BO	CMP	Both	2	1	1	A
11/14/2017	MO	2D/3D	400	22	11	11	A
11/14/2017	MO	2D/3D	900	22	11	11	A
11/14/2017	MO	CMP	Both	2	1	1	U
11/16/2017	MO	2D/3D	400	22	11	11	A
11/16/2017	MO	2D/3D	900	22	11	11	A
11/16/2017	MO	CMP	Both	2	1	1	U
11/18/2017	MO	2D/3D	400	22	11	11	A
11/18/2017	MO	2D/3D	900	22	11	11	A
11/18/2017	MO	CMP	Both	2	1	1	U
11/20/2017	MO	2D/3D	400	22	11	11	A
11/20/2017	MO	2D/3D	900	22	11	11	A
11/20/2017	MO	CMP	Both	2	1	1	U
11/22/2017	MO	2D/3D	400	22	11	11	A
11/22/2017	MO	2D/3D	900	22	11	11	A
11/22/2017	MO	CMP	Both	2	1	1	U
11/24/2017	MO	2D/3D	400	22	11	11	A
11/24/2017	MO	2D/3D	900	22	11	11	A
11/24/2017	MO	CMP	Both	2	1	1	U
12/3/2017	DO	2D/3D	400	42	21	21	U
12/3/2017	DO	2D/3D**	900	21	11	10	U
12/3/2017	DO	CMP	Both	2	1	1	U

I. Buried Objects SIte Results

The soil horizons identified within the open trench independently confirmed the soil profile from Web Soil Survey (USDA NRCS, 2017). The horizons at this site suggest that the Bama series soil is present with a taxonomic class of fine-loamy, siliceous, thermic Typic Paleudult (Table 2). Confirming soil taxonomy is necessary to understand the level of attenuation from the GPR antennas in the resulting data. The profile was observed from the north side of the trench where soil horizons could be identified from a flat soil surface (Figure 15). The profile presented three distinct horizons with the top layer being highly disturbed, indicative of a plowed zone.

Figure 15. Soil profile from within the backhoe trench at EV Smith Research Center (approx. 1.9 m deep). Dotted black line indicates boundary between first (Ap) and second (Bt1) horizons.

Table 2: Soil Description: EV Smith 1

Soil Horizon	Depth (cm)	Description
Ap	0 to 50	brown (7.5 YR 4/4) loamy sand; weak moderate sub-angular blocky structure; very friable; common fine roots found at 18 cm; moderate rounded gravel(1-4 cm); 10% clay; clear wavy boundary
Bt1	50 to 110	dark red (2.5 YR 3/6) sandy clay loam; weak moderate sub-angular blocky; friable; common rounded gravel (0.5-6 cm); 20% clay; gradual wavy boundary
Bt2	110 +	strong brown (7.5 YR 4/6) and dark red (2.5 YR 3/6) sandy clay loam; weak moderate sub-angular blocky; friable; many rounded gravel (0.5 – 5cm); 25% clay

The observed profile is similar in characteristics to the BAMA series soil as mapped from Web Soil Survey (Figure 8). While it is different from the typical expression of soil horizons, missing a distinguishable B or BE horizon, it does correlate to the range in characteristic description, including quartz gravel throughout solum, alternate Bt hue, value and chroma, and relict redoximorphic features in the lower profile.

Since the objective was to resolve buried objects in the subsurface, the 2D profiles with the 400 MHz antenna and 900 MHZ antennas were analyzed. CMP data failed to show any returns at this location and therefore were abandoned. The spacing of the acquisition lines at the trench was 0.3 m, resulting in a total of 47 profile lines for the 400 MHz survey and 11 for the 900 MHz. Of the 900 MHz lines that produced reflections, a couple of lines confirmed observed reflections in the 400 MHz survey (Figure 16-18).

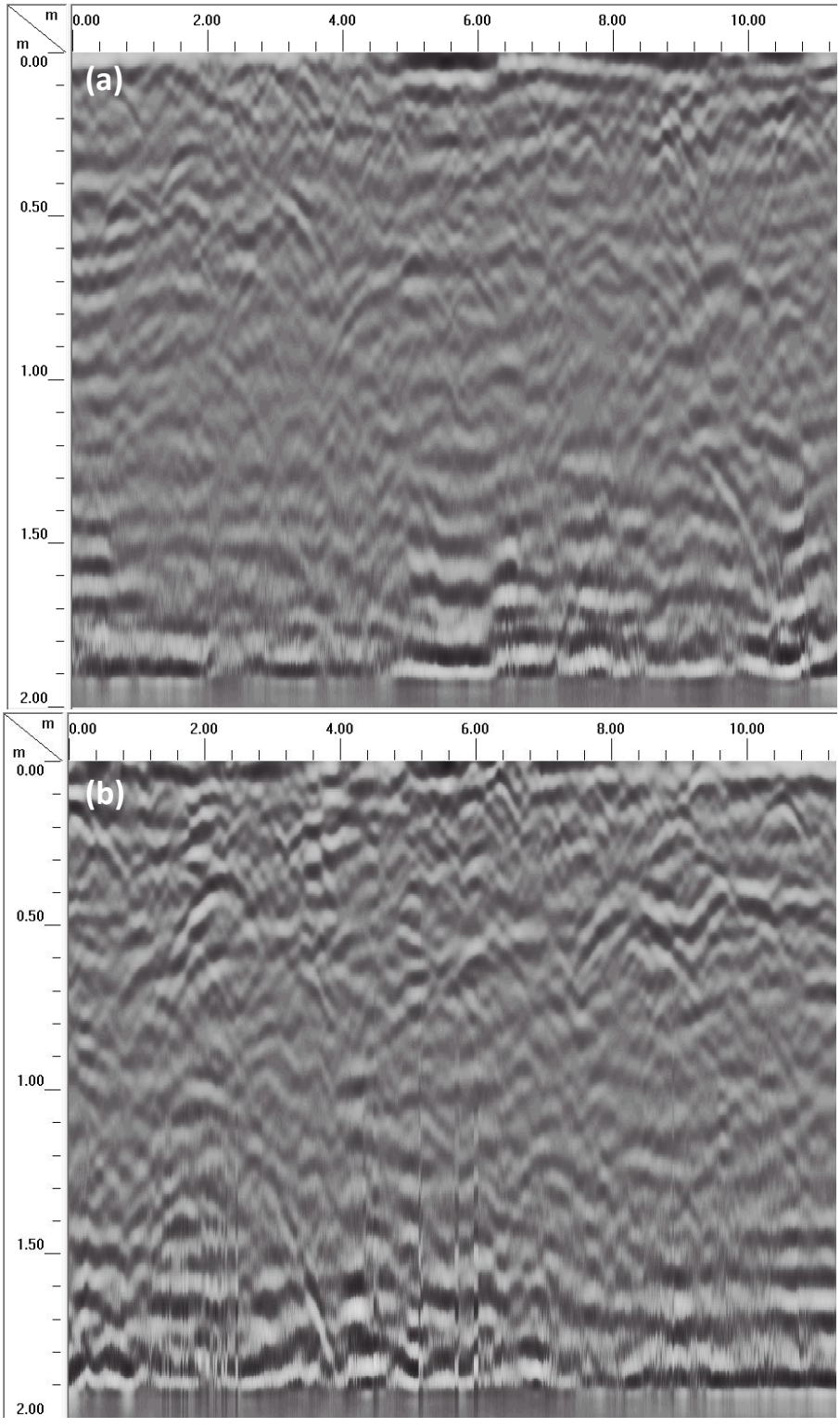

Figure 16. Two GPR lines with time-zero and background filters run parallel to each other: (a) line 006 and (b) line 007. Both lines are N-S oriented and were taken in opposite directions and are GPR profiles that do not show distinct reflections.

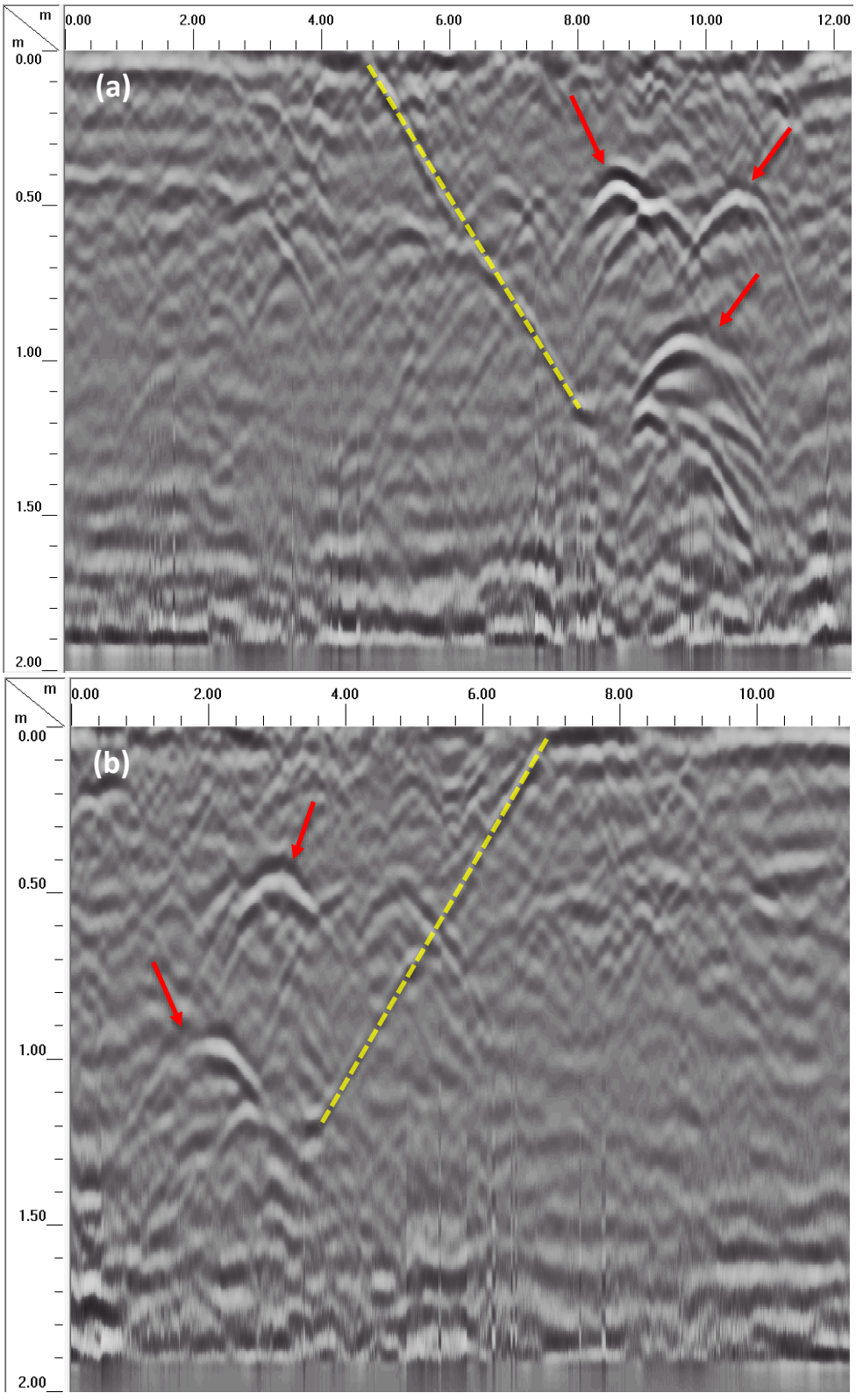

Figure 17. Two GPR lines with time-zero and background filters run parallel to each other: (a) line 008 and (b) line 009. Both lines are N-S facing and were taken in opposite directions. Arrows point to distinct reflections interpreted to be rebar. The dotted line indicates the boundary between the disturbed and undisturbed sediment in the trench.

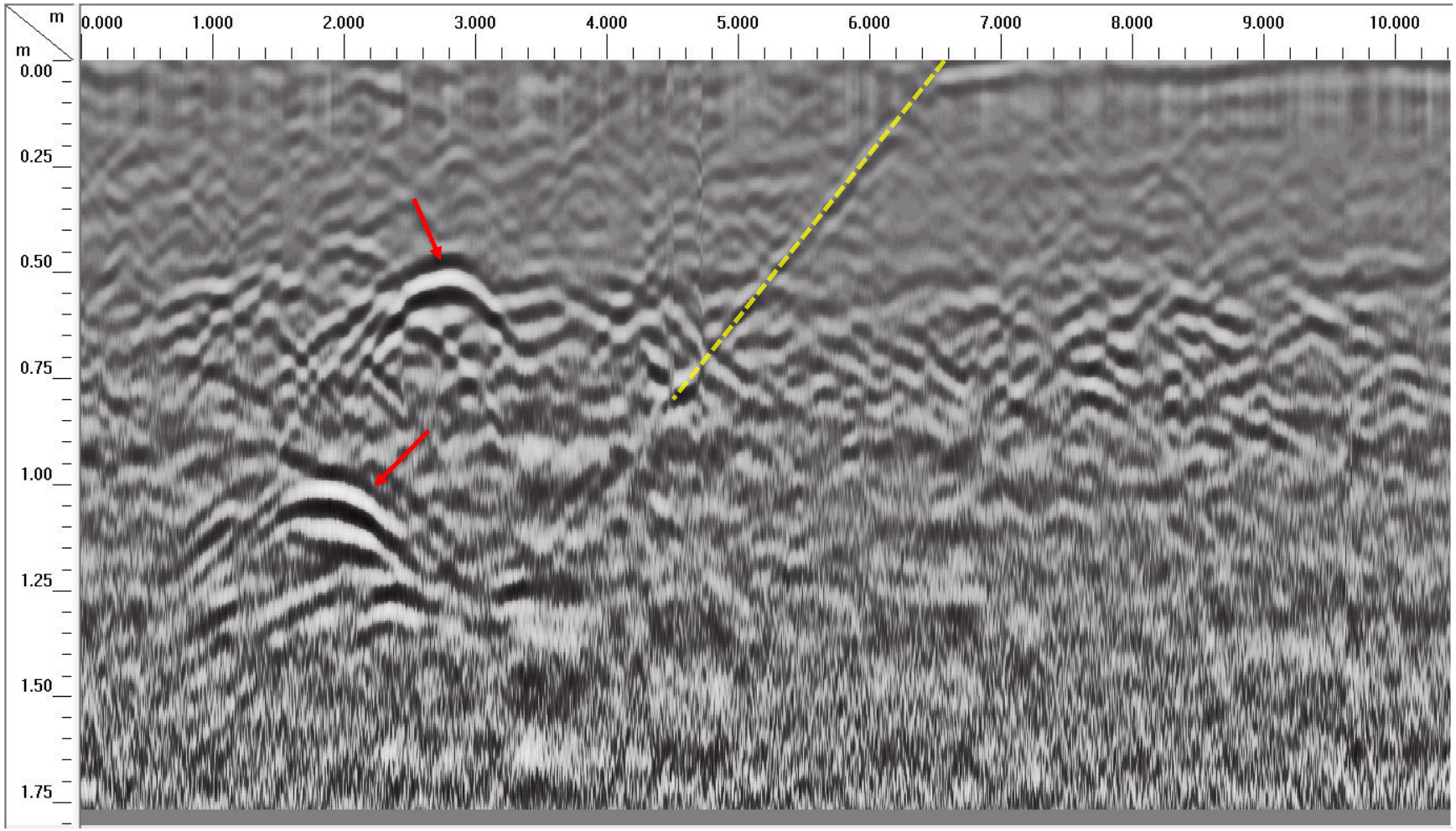

Figure 18. 2D GPR line (006) taken with the 900 MHZ antenna,processed using time-zero and background filters. The dotted line indicates the boundary between the disturbed and undisturbed sediment in the trench. Arrows indicate strong target return reflections that are likely from the buried rebar.

The two most successful transect lines from the 2D GPR survey using the 400 MHz antenna were lines 008 and 009. Profiles from lines 008 and 009 display multiple hyperbolas (Figure 17) that are interpreted as rebar (due to its high RDP). The rebar placement is confirmed by a 900 MHz GPR profile (Figure 18), with depths that correlate to the trench depths measured in the field. Line (006) from the 900 MHz survey has the same placement and depths as the (009) line from the 400 MHZ survey. The indicated hyperbolas (red arrows) match the depths of placed rebar at approximately 0.50 m and 1.9 m corresponding to *in-situ* measurements. Due to the drastic difference in RBD between the host soil and the metal rebar, the hyperbola reflections are strong within each profile. The trench boundary (yellow dotted line) is confirmed in at least three profiles from both 400 and 900 MHz surveys. This indicates that the reflections identified are the undisturbed/ disturbed sediment boundary, not an artifact from acquisition or post-processing. In comparison, unsuccessful lines (006 and 007) from the 400 MHz survey (Figure 16) have faint hyperbolas but when processed for migration those traces disappear indicating that the faint hyperbolas are reflections from non-targets in the subsurface (pebbles, buried stumps, etc.).

Hyperbolas are evident in the above profiles that are orientated N-S, perpendicular to the placement of the rebar and other buried objects. The E-W profiles did not show hyperbolic reflections, indicating that transects set up perpendicular to buried targets achieve maximum chance of detection. The trench boundary was resolved by GPR using both antennas because their wavelengths were smaller than the boundary interface. Due to the close placement of all buried objects, and the varying degree of materials, sizes and depths of objects all returns except those of rebar were either too small to distinguish or had no identifiable return. While

only one material within the trench was resolved, such intense reflections and the identification of the trench boundary within a clay-rich soil is promising for the future use of GPR in coastal plain sediments.

II. Turfgrass Plot Moisture Results

Results from the turfgrass plot indicate that drying from origianl saturation occurred November 14 to November 24, 2017. Parameters including wet sediment (m_{wet}), dry sediment (m_{dry}), mass of water (m_{water}), gravimetric water (θ_g), volumetric water, and bulk density were all calculated from auger samples (Table 3 and 4). These parameters were used to calculate gravimetric and volumetric water content at two depths per day of data collection. Volumetric water content (θ_v) was converted to percent for comparison to POGO measurements. The POGO meter was used to confirm that auger measurements are an accurate method for moisture content sampling. POGO measurements show a decrease in surface moisture content, with some fluctuations, between the beginning and end of the experiment (Table 5).

Table 3. Summary of lab calculations on auger samples taken from the turfgrass moisture plot and one sample taken at D'Olive Creek. (DH= down hole depth [approx. 6 cm for all surface measurements], surface=within 7 cm of the surface)

Date	Sampling depth (cm)	Beaker weight (g)	Beaker + sediment (m_{wet}) (g)	Beaker + sediment (m_{dry}) (g)	Sediment (m_{dry}) (g)	$m_{water=}$ m_{wet}-m_{dry} (g)
11/14/2017	surface (~6 cm)	127.13	329.57	305.17	178.038	24.4
11/14/2017	DH 56 cm	130.02	327.28	304.37	174.3479	22.91
11/16/2017	surface	128.26	320.75	300.7	172.44	20.05
11/16/2017	DH 67 cm	127.13	306.97	293.22	166.09	13.75
11/18/2017	surface	128.52	314.47	293.66	165.14	20.81
11/18/2017	DH 53 cm	126.43	326.55	309.51	183.08	17.04
11/20/2017	surface	126.63	317.90	296.31	169.68	21.59
11/20/2017	DH 60 cm	128.94	323.96	307.5	178.56	16.46
11/22/2017	surface	128.12	318.52	296.19	168.07	22.33
11/22/2017	DH 56 cm	128.77	326.73	311.19	182.42	15.54
11/24/2017	surface	129.51	316.11	295.86	166.35	20.25
11/24/2017	DH 64 cm	127.32	312.43	299.35	172.03	13.08

Table 4. Summary of calculated gravimetric and volumetric water content of each sample. Volumetric water content (θ_v) was then converted to volumetric water content %.

Date	Gravimetric (θ_g)	Gravimetric (%)	Volumetric (θ_v)	Volumetric %
11/14/2017	0.137049394	13.70493939	0.264384007	26.43840069
11/14/2017	0.131403934	13.14039343	0.248239246	24.82392459
11/16/2017	0.116272327	11.62723266	0.217249973	21.72499729
11/16/2017	0.082786441	8.278644109	0.148986889	14.89868892
11/18/2017	0.126014291	12.60142909	0.225484885	22.54848846
11/18/2017	0.093074066	9.307406598	0.184635388	18.46353884
11/20/2017	0.12723951	12.72395097	0.233936504	23.39365045
11/20/2017	0.0921819	9.218189964	0.178350851	17.83508506
11/22/2017	0.132861308	13.28613078	0.241954708	24.1954708
11/22/2017	0.085188028	8.518802763	0.168382273	16.83822733
11/24/2017	0.121731289	12.17312894	0.219417055	21.94170549
11/24/2017	0.07603325	7.603325001	0.141727164	14.17271644

Soil Moisture Analysis

There was one minor rainfall event on November 19, 2017 of 0.12 inches. To account for rainfall affecting moisture content measurements, gravimetric water content was plotted with rainfall occurance (Figures 19 and 20). Auger samples from the surface and at depth have the most significant drop in moisture after 48 hours from original saturation. Although moisture content has a significant intitial drop, it increases slightly from November 16 to November 22. This could be from changing biological activity dependent on moisture flucuations and temperature during the night and in the early mornings that affect meter readings (Orchard and Cook, 1983). Most surveys were done between 11 am and 4 pm, so the dew could have infiltrated the first couple cm of the surface, altering surface measurements. Mositure content continues to increase after the rain event (0.12 inches) on November 19, 2017.

Auger moisture measurements at depth also drop during the first 48 hours and then level out during the course of the experiment. This may indicate that fluctuations of surface moisture are more sesnsitive to rainfall compared to those taken at depth, but more data is needed to determine this a factor. The rain event does not seem to have an effect on moisture content at approximately 57 cm, which is expected due to the small amount of rainfall. The converted volumetric water content measurements follow the same trend as the gravimetric water content data (Figures 21 and 22).

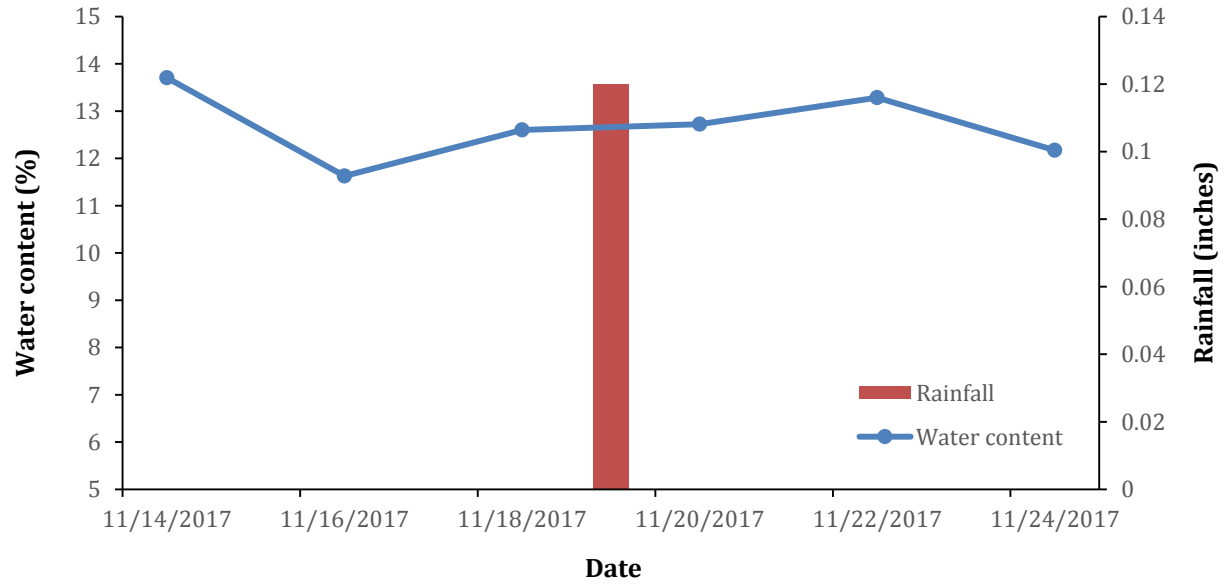

Figure 19. Gravimetric water content derived from the surface of an auger hole measured at the turfgrass plot. Rainfall of 0.12 inches occurred on November 19th, 2017, in between two days of taking data.

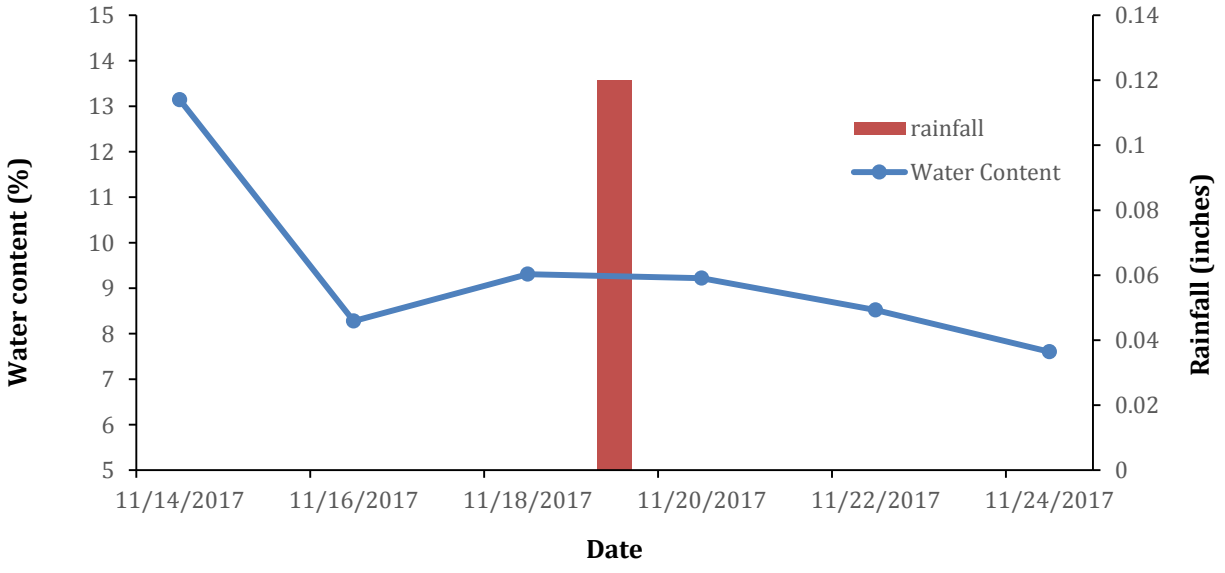

Figure 20. Gravimetric water content derived from depth within an auger hole (same hole in Figure 19) on the turfgrass plot. Rainfall of 0.12 inches occurred on November 19th, 2017, in between two days of taking data.

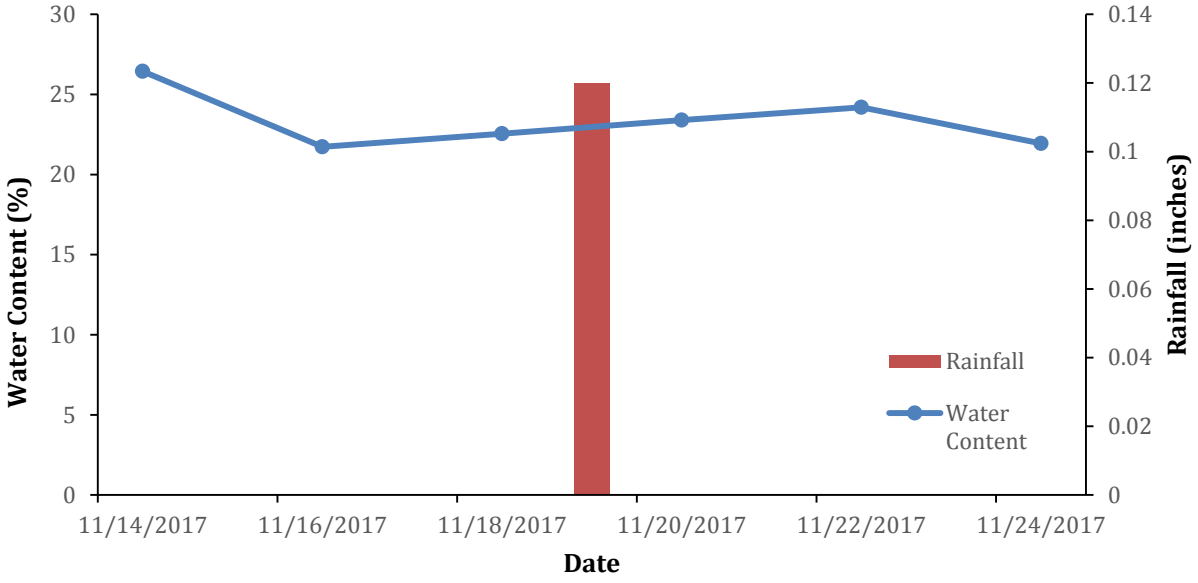

Figure 21. Volumetric water content from the surface at the turfgrass plot, calculated from gravimetric water content and volume of the sampling canister.

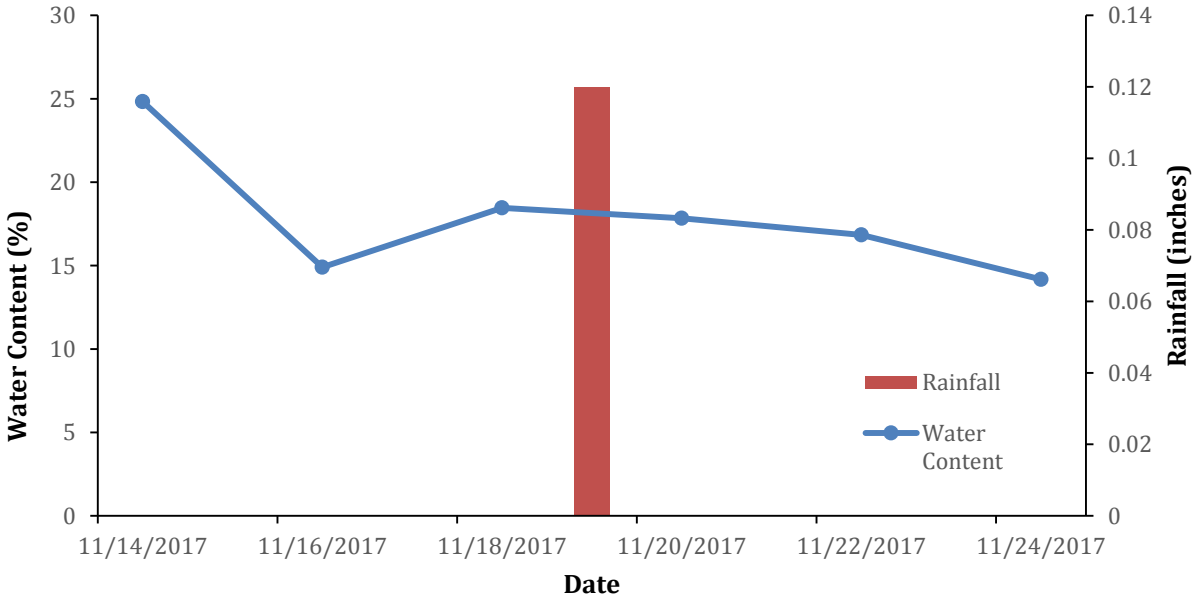

Figure 22. Volumetric water content from ~57 cm depth at the turfgrass plot, calculated from gravimetric water content and volume of the sampling canister.

The POGO measurements plotted with the rainfall event indicate that the east, north and middle sampling locations (Figure 12) may have responded to the small rainfall amount on November 19, 2017 (Table 5). While the auger surface measurement was taken between 0-7 cm, the POGO measurements are taken within the first centimeter of the surface. It was expected that the POGO would pick up the rainfall event at the surface, but evapotranspiration may have removed moisture before data were taken on November 20, 2017 (Orchard and Cook, 1983).

Similar trends are repeated in the volumetric water content data. The gravimetric surface measurement before the rainfall event seems to plateau then increase due to the rain while the volumetric conversion removes that plateau and indicates that moisture content was rising before the rain. Since the gravimetric data was calucated from mass it may be more accurate but cannot be directly compared to the POGO surface measurements.

Since the rainfall event occurred on a day that moisture and GPR data were not taken, it is possible that the POGO measurement prong depth did not exceed the depth at which surface moisture was being stored, while the auger measurement did. Because gravimetric readings are based on mass and not direct volume, it is possible that the gravimetric readings were more inclusive of moisture content below 1 cm of the surface.

POGO meter measurements plotted with the surface auger hole measurements confirm that moisture has a significant drop between the first and third day of drying and plateaus soon after. There are slight variations dependent on location of the POGO measurement as well. The closest POGO measurement to auger hole sampling was the south side of the grid. The south side and surface auger hole measurements have a similar trend but the moisture percent varies

between the two. Overall, it appears that moisture content measured by both POGO meter and auger hole samples are predictive for general moisture content analysis.

Table 5. POGO meter measurements taken on the northern boundary of the 10m x 10m plot at the turfgrass unit. Averages were used in Figure 23 and 24. Each sample was taken three times every two days for accuracy.

Date	Location	Sample #	Moisture %	Temp ˚C	Temp ˚F	Average Moisture (%)	Average Temp ˚C
11/14/2017	N	1	30.00	33.10	91.60	28.87	31.96
11/14/2017	N	2	29.50	32.10	89.70		
11/14/2017	N	3	27.10	30.70	87.30		
11/16/2017	N	1	20.40	24.40	75.90	22.30	24.03
11/16/2017	N	2	22.30	24.20	75.50		
11/16/2017	N	3	24.20	23.50	74.30		
11/18/2017	N	1	22.60	21.30	70.30	21.03	21.43
11/18/2017	N	2	20.60	21.50	70.70		
11/18/2017	N	3	19.90	21.50	70.70		
11/20/2017	N	1	24.30	19.30	66.80	21.70	19.30
11/20/2017	N	2	22.00	19.30	66.80		
11/20/2017	N	3	18.80	19.30	66.80		
11/22/2017	N	1	20.60	13.80	56.90	22.17	13.96
11/22/2017	N	2	22.80	14.10	57.40		
11/22/2017	N	3	23.10	14.00	57.20		
11/24/2017	N	1	21.40	24.40	75.90	22.33	23.86
11/24/2017	N	2	21.80	23.50	74.30		
11/24/2017	N	3	23.80	23.70	74.70		

Table 6. POGO meter measurements taken in the center of the 10m x 10m plot at the turfgrass unit. Averages were used in Figure 23 and 24. Each sample was taken three times, every two days for accuracy.

Date	Location	Sample #	Mositure %	Temp ˚C	Temp ˚F	Average Moisture (%)	Average Temp ˚C
11/14/2017	M	4	26.30	28.60	83.50	25.40	28.23
11/14/2017	M	5	28.20	28.30	83.00		
11/14/2017	M	6	21.70	27.80	82.00		
11/16/2017	M	4	15.20	23.30	73.90	17.63	23.03
11/16/2017	M	5	21.00	23.00	73.40		
11/16/2017	M	6	16.70	22.80	73.00		
11/18/2017	M	4	16.40	21.50	70.70	18.07	21.43
11/18/2017	M	5	16.60	21.50	70.70		
11/18/2017	M	6	21.20	21.30	70.30		
11/20/2017	M	4	17.30	19.30	66.80	14.90	19.30
11/20/2017	M	5	14.30	19.30	66.80		
11/20/2017	M	6	13.10	19.30	66.80		
11/22/2017	M	4	16.40	14.30	57.70	18.03	14.33
11/22/2017	M	5	16.70	14.30	57.70		
11/22/2017	M	6	21.00	14.40	58.00		
11/24/2017	M	4	15.90	23.70	74.70	20.07	23.56
11/24/2017	M	5	19.70	23.50	74.30		
11/24/2017	M	6	24.60	23.50	74.30		

Table 7. POGO meter measurements taken on the southern boundary of the 10m x 10m plot at the turfgrass unit. Averages were used in Figure 23 and 24. Each sample was taken three times, every two days for accuracy.

Date	Location	Sample #	Moisture %	Temp ˚C	Temp ˚F	Average Moisture (%)	Average Temp ˚C
11/14/2017	S	7	33.00	27.80	82.00	31.83	26.96
11/14/2017	S	8	32.10	26.70	80.00		
11/14/2017	S	9	30.40	26.40	79.50		
11/16/2017	S	7	24.20	22.10	71.90	24.67	21.96
11/16/2017	S	8	23.20	22.10	71.90		
11/16/2017	S	9	26.60	21.70	71.10		
11/18/2017	S	7	24.00	21.50	70.70	23.53	21.50
11/18/2017	S	8	24.80	21.50	70.70		
11/18/2017	S	9	21.80	21.50	70.70		
11/20/2017	S	7	25.30	19.50	67.10	23.67	19.43
11/20/2017	S	8	23.50	19.30	66.80		
11/20/2017	S	9	22.20	19.50	67.10		
11/22/2017	S	7	24.10	14.90	58.80	23.73	15.10
11/22/2017	S	8	23.70	15.20	59.40		
11/22/2017	S	9	23.40	15.20	59.40		
11/24/2017	S	7	23.60	23.30	73.90	23.97	23.20
11/24/2017	S	8	23.80	23.30	73.90		
11/24/2017	S	9	24.50	23.00	73.40		

Table 8. POGO meter measurements taken on the eastern boundary of the 10m x 10m plot at the turfgrass unit. Averages were used in Figure 23 and 24. Each sample was taken three times, every two days for accuracy.

Date	Location	Sample #	Moisture %	Temp ˚C	Temp ˚F	Average Moisture (%)	Average Temp °C
11/14/2017	E	10	27.60	25.90	78.60	25.93	25.63
11/14/2017	E	11	26.90	25.40	77.70		
11/14/2017	E	12	23.30	25.60	78.20		
11/16/2017	E	10	20.40	21.10	70.00	19.83	21.03
11/16/2017	E	11	18.40	21.10	70.00		
11/16/2017	E	12	20.70	20.90	69.60		
11/18/2017	E	10	15.20	21.50	70.70	19.17	21.50
11/18/2017	E	11	21.30	21.50	70.70		
11/18/2017	E	12	21.00	21.50	70.70		
11/20/2017	E	10	18.20	19.30	66.80	19.00	19.43
11/20/2017	E	11	18.70	19.50	67.10		
11/20/2017	E	12	20.10	19.50	67.10		
11/22/2017	E	10	23.60	15.40	59.60	21.83	15.43
11/22/2017	E	11	21.00	15.20	59.40		
11/22/2017	E	12	20.90	15.70	60.20		
11/24/2017	E	10	22.50	23.00	73.40	20.07	22.86
11/24/2017	E	11	19.60	22.60	72.60		
11/24/2017	E	12	18.10	23.00	73.40		

Table 9. POGO meter measurements taken on the western boundary of the 10m x 10m plot at the turfgrass unit. Averages were used in Figure 23 and 24. Each sample was taken three times, every two days for accuracy.

Date	Location	Sample #	Moisture %	Temp ˚C	Temp ˚F	Moisture Average	Temp °C Average
11/14/2017	W	13	30.10	24.90	76.80	28.13	24.83
11/14/2017	W	14	28.10	24.90	76.80		
11/14/2017	W	15	26.20	24.70	76.40		
11/16/2017	W	13	21.10	20.70	69.20	20.83	20.50
11/16/2017	W	14	22.00	20.70	69.20		
11/16/2017	W	15	19.40	20.10	68.20		
11/18/2017	W	13	21.00	21.70	71.10	20.80	21.70
11/18/2017	W	14	23.10	21.70	71.10		
11/18/2017	W	15	18.30	21.70	71.10		
11/20/2017	W	13	19.80	19.50	67.10	19.27	19.43
11/20/2017	W	14	18.30	19.30	66.80		
11/20/2017	W	15	19.70	19.50	67.10		
11/22/2017	W	13	18.50	15.70	60.20	18.77	15.96
11/22/2017	W	14	20.20	16.00	60.80		
11/22/2017	W	15	17.60	16.20	60.80		
11/24/2017	W	13	19.70	22.80	73.00	21.17	22.80
11/24/2017	W	14	21.40	22.80	73.00		
11/24/2017	W	15	22.40	22.80	73.00		

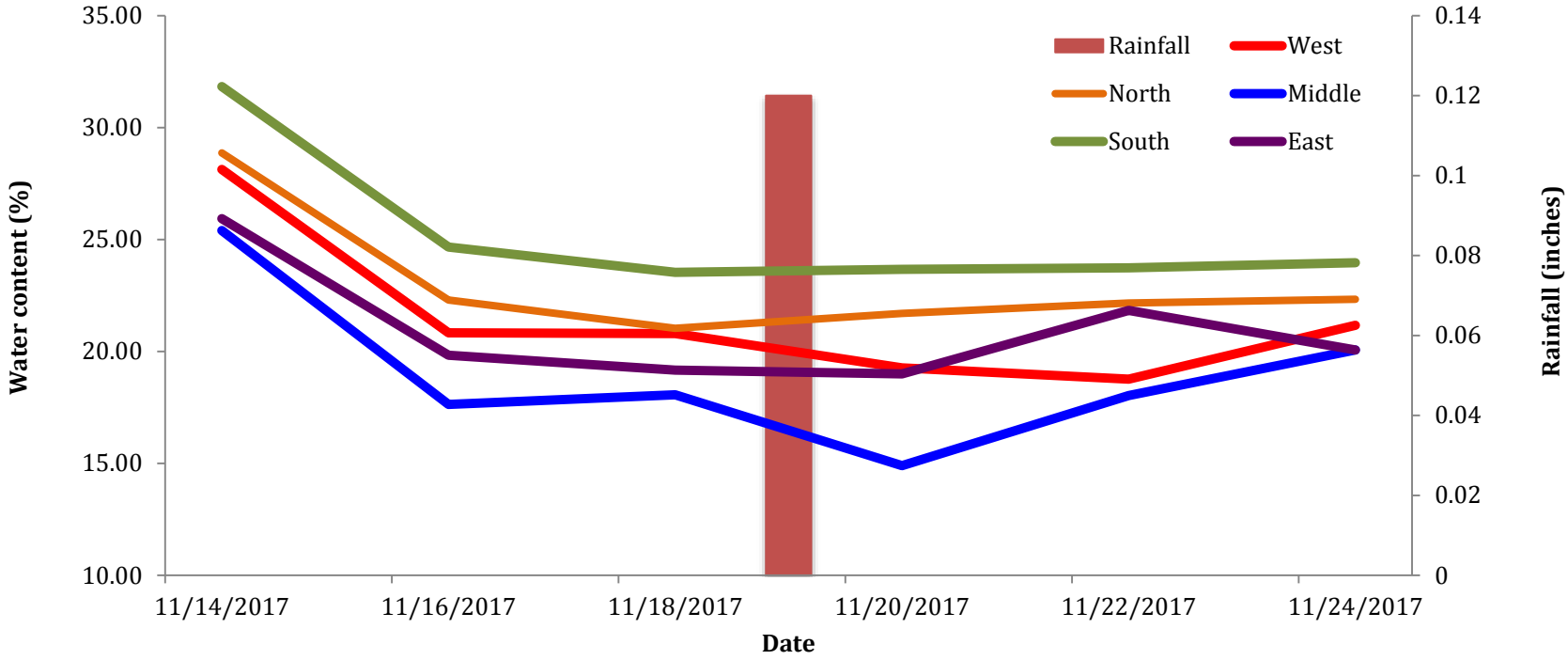

Figure 23. Volumetric water content by percent taken using a POGO meter measure on the surface of the turfgrass plot. Each location has daily averages that were plotted for every two days during the experiment.

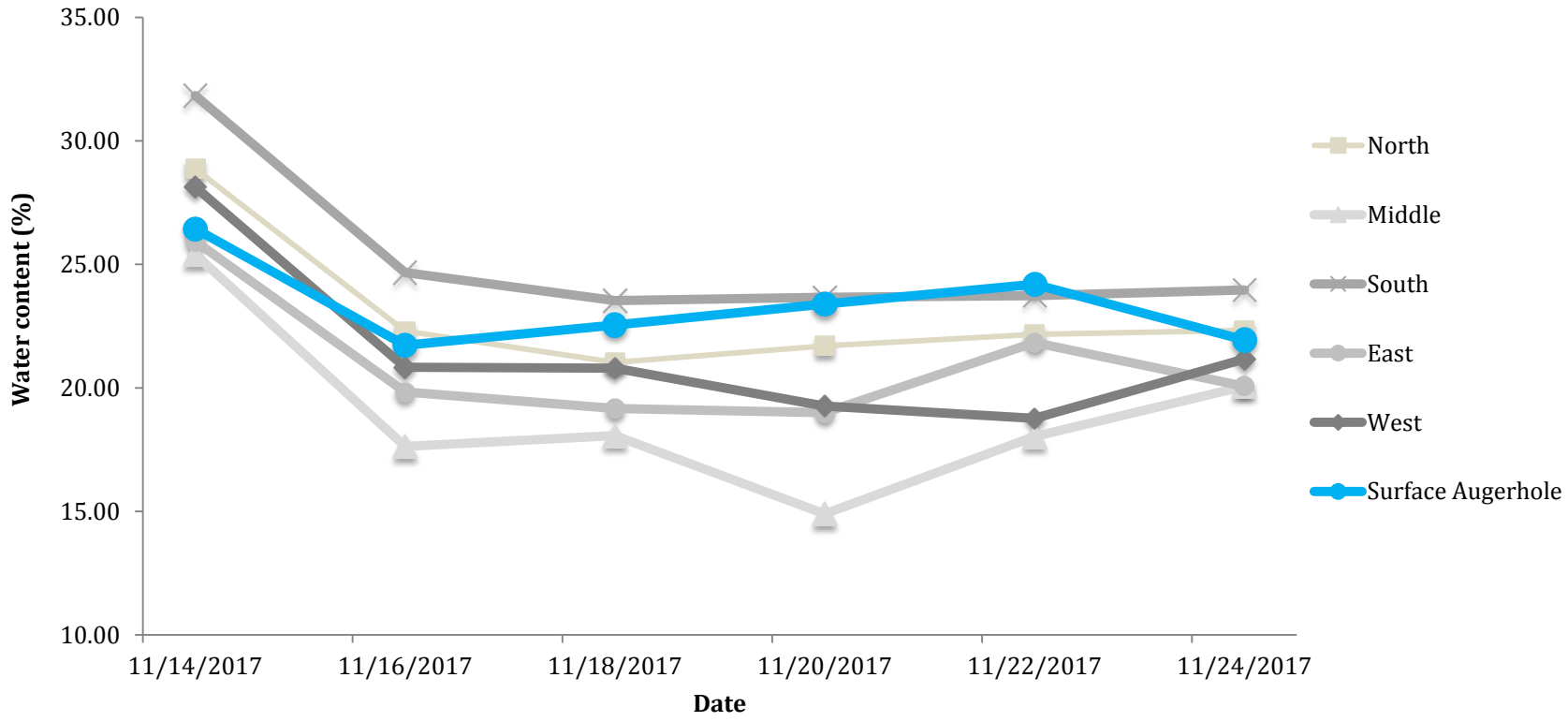

Figure 24. Volumetric water content by percent taken using a POGO meter measure on the surface of the turfgrass plot. Each location has daily averages that were plotted for every two days during the experiment.

Velocity Analysis

Velocities calculated from the turfgrass plot CMP data were used to determine if the shallow subsurface is drying over time (Figures 25 and 26). The slope of a line formed from first distinct arrival on each trace on each profile gives an estimated velocity that can then be used to infer changes in moisture. Due to behavior of radar waves, if the moisture content decreases velocity increase. These two profiles depict the lines fitted to the first arrival wave that were averaged for a velocity. The level of error associated with estimating a velocity is assumed to be high due to the variability in picking and occasionally the ability to distinguish the initial return from noise within the profile. Since picking velocity phases is subjective, three possible fits to the first arriving wave were made and the average of the slopes was used as the velocity for the profile. Closer spacing in CMP increments would increase resolution and allow for a better estimation of velocity. The velocity for each profile was estimated and the time of the first reflection was recorded. This was taken to determine if one way travel time to reflectors in the subsurface (Figure 27). Wave propagation is measured as two-way travel time (Table 10).

It appears that line 1 may have detected a horizontal horizon around 0.8 m but since line 2 does not have any consistent depths it is unlikely that either are detecting a continuous, resolvable layer (Figure 26). Since there were no pre-determined targets buried at this site, it is almost impossible to independently confirm subsurface reflections and possible horizons.

Velocities plotted in Figure 28 show an increasing trend of velocity increasing as the plot dries. It appears that the rainfall event did have a small, immediate effect on CMP velocity, seen in the slight dip in velocity on November 20th. The rapid increase between 0.09186667 m/ns and 0.10553333 m/ns on November 20th through November 22nd indicates that water content

may have decreased significantly between the two days. During these same dates measured volumetric water content follows a plateau of moisture content at the surface with a small decrease in water content at depth.

Volumetric moisture content from auger measurements plotted against velocities in Figure 29 and 30 indicate that there is little to no correlation between soil moisture and velocity changes. Specifically, there seems to be no correlation between surface moisture content and velocity (Figure 29), while Line 1 and 2 do have higher R^2 values for soil moistures values at depth (Figure 30). Due to a lack of quantitative data connecting the relationship of moisture content from volumetric water content and CMP data, it is difficult to conclude that a small change in measured water content drives a large velocity change in GPR data. The dataset is not robust enough to draw conclusions between the relationship of moisture content and velocity without more testing. With continued testing, a direct correlation between volumetric water content and CMP may be determined to help estimate moisture content trends over time.

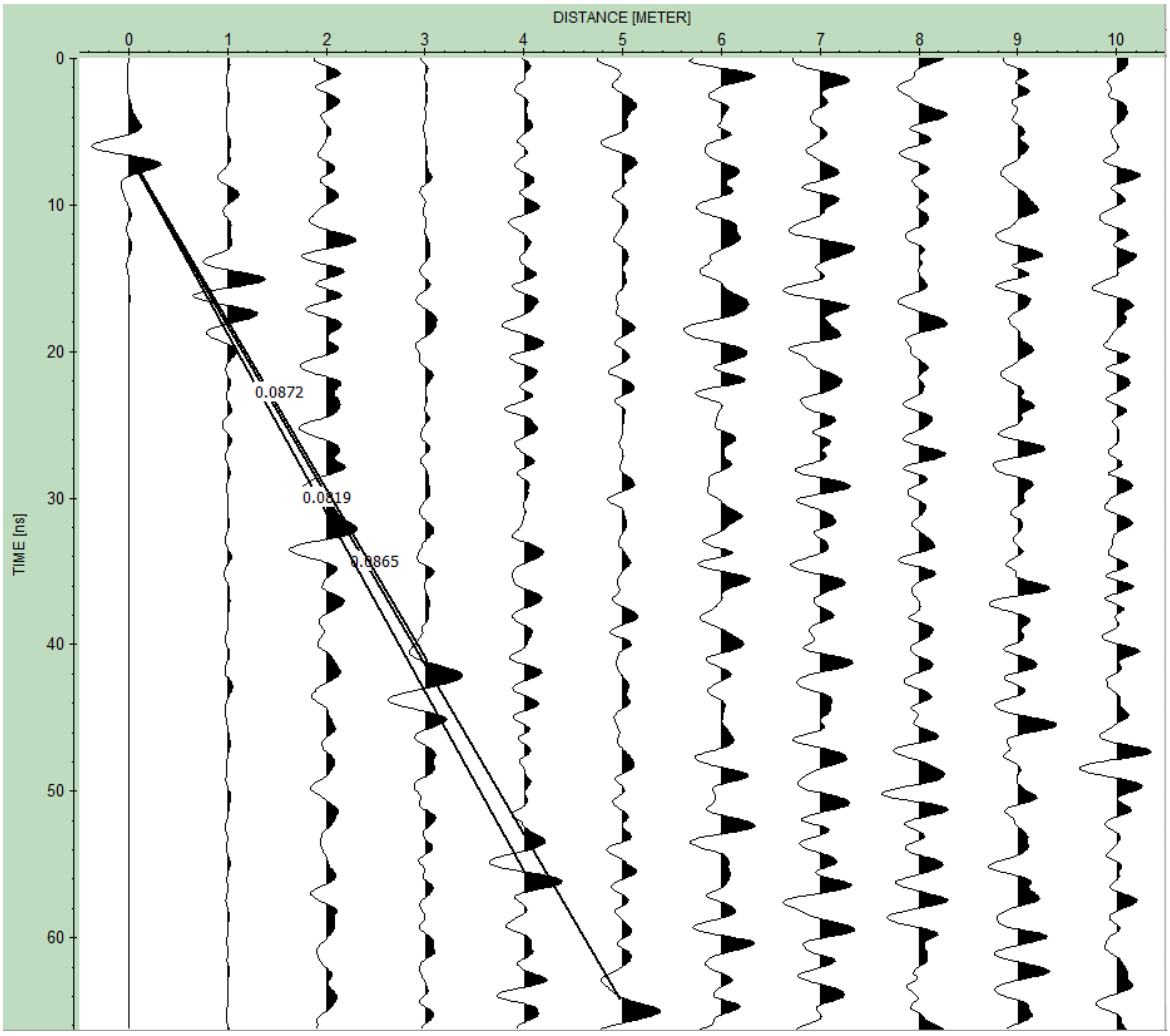

Figure 25. November 11, 2017 Line 1 CMP data processed with band-pass and energy-decay filters. Black lines are fitted to an arriving phase for velocity analysis within ReflexW™. First arrival reflections are identifiable to meter 5.

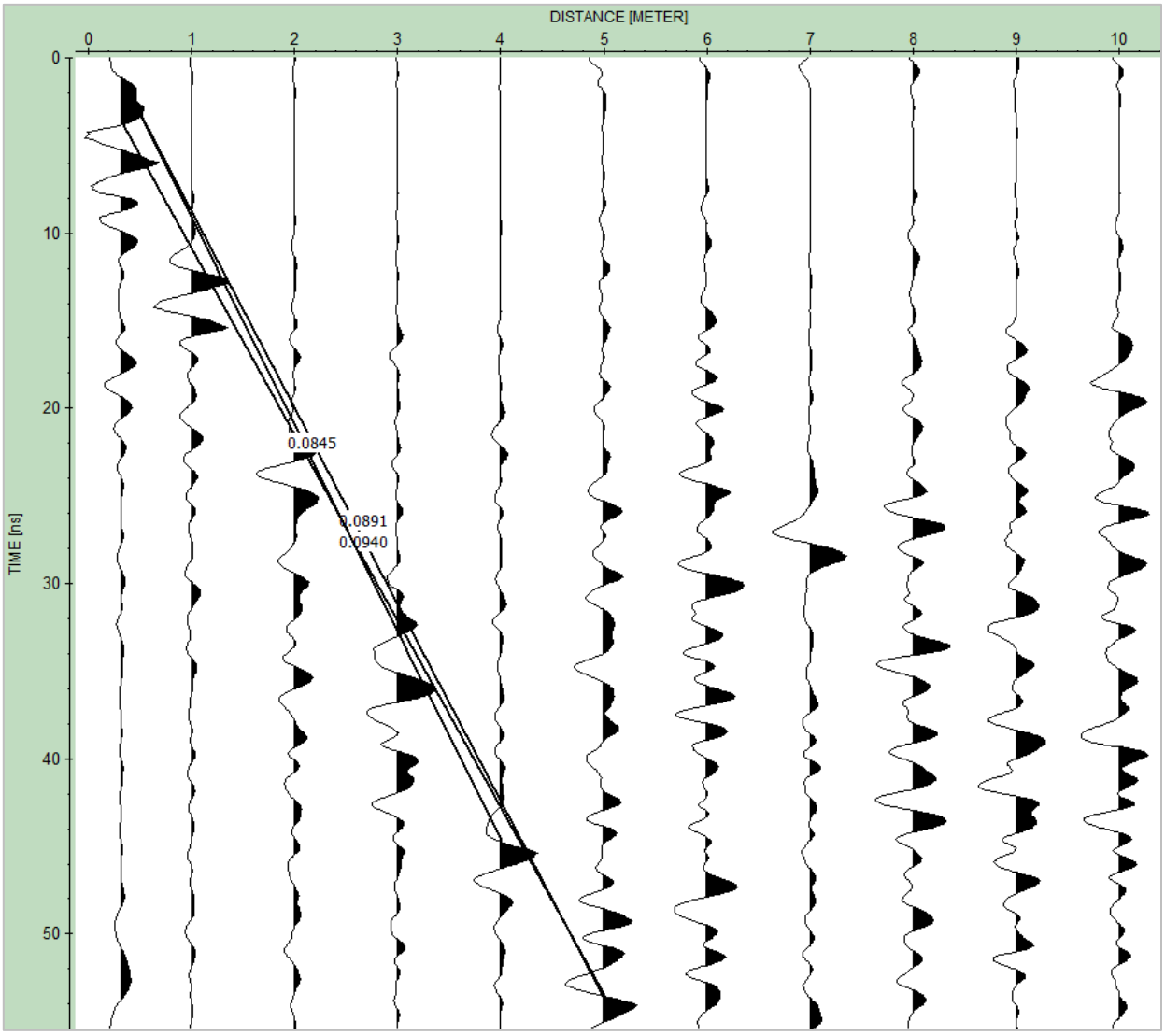

Figure 26. November 24, 2017 Line 1 CMP data processed with band-pass and energy-decay filters. Black lines are fitted to an arriving phase for velocity analysis within ReflexW™. First arrival reflections are identifiable to meter 5.

Table 10. Velocity data for the turfgrass plot along two CMP lines modeled in Figure 12.

Date	Line	Velocity (m/ns)	Time (ns)
11/14/2017	1	0.08323333	18.6
11/14/2017	2	0.0865	20.1
11/16/2017	1	0.09266667	17.6
11/16/2017	2	0.09176667	13.6
11/18/2017	1	0.09546667	17.3
11/18/2017	2	0.0908	20.5
11/20/2017	1	0.09186667	17.1
11/20/2017	2	0.09263333	10.4
11/22/2017	1	0.10553333	17.7
11/22/2017	2	0.11283333	15.2
11/24/2017	1	0.0892	16.6
11/24/2017	2	0.0889	19.3

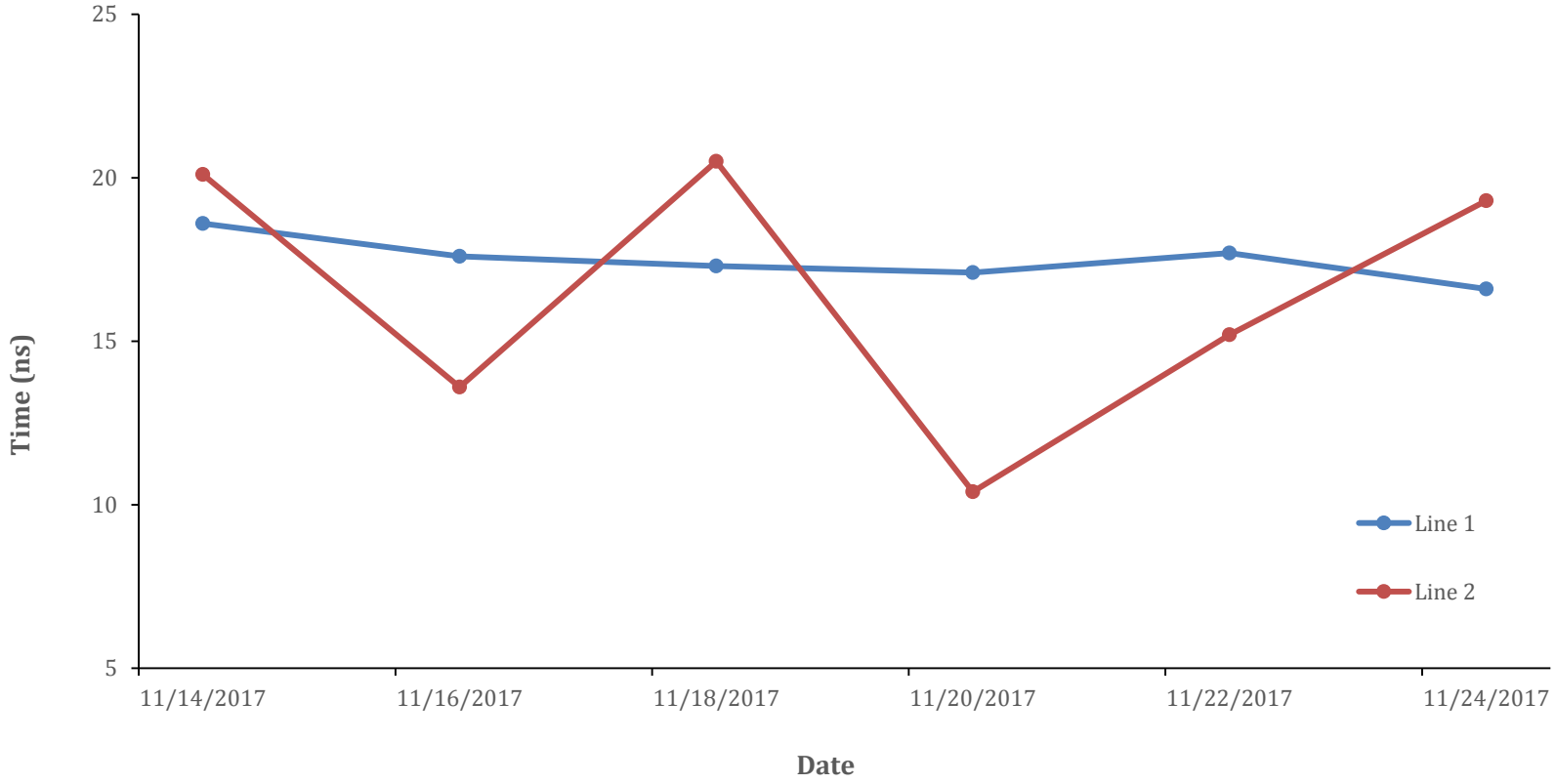

Figure 27. Depth into the subsurface for both Line 1 and Line 2 surveyed at the Turfgrass plot depicting any continuous horizontal layers.

Figure 28. Average velocities for both line 1 and 2 over two weeks at turfgrass plot. Blue = line 1 (oriented E-W), red = line 2 (orientated N-S), green bar represents rainfall.

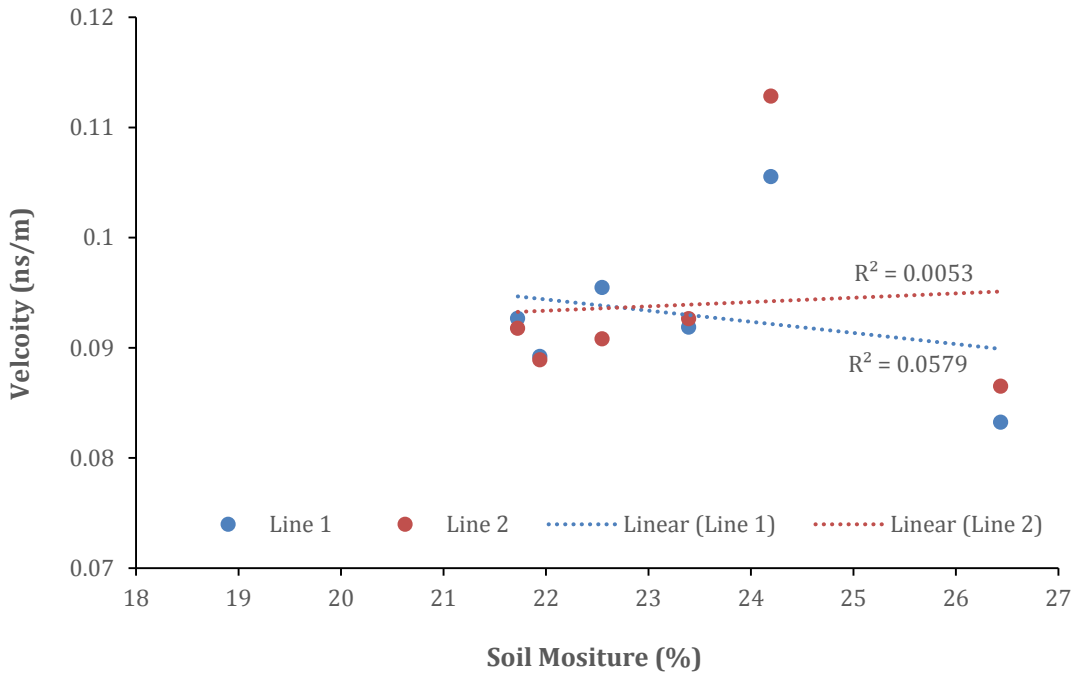

Figure 29. Scatter plot of surface soil moisture (auger data) and velocity for each CMP line from the turfgrass moisture plot. A linear regression for each determines R^2 value.

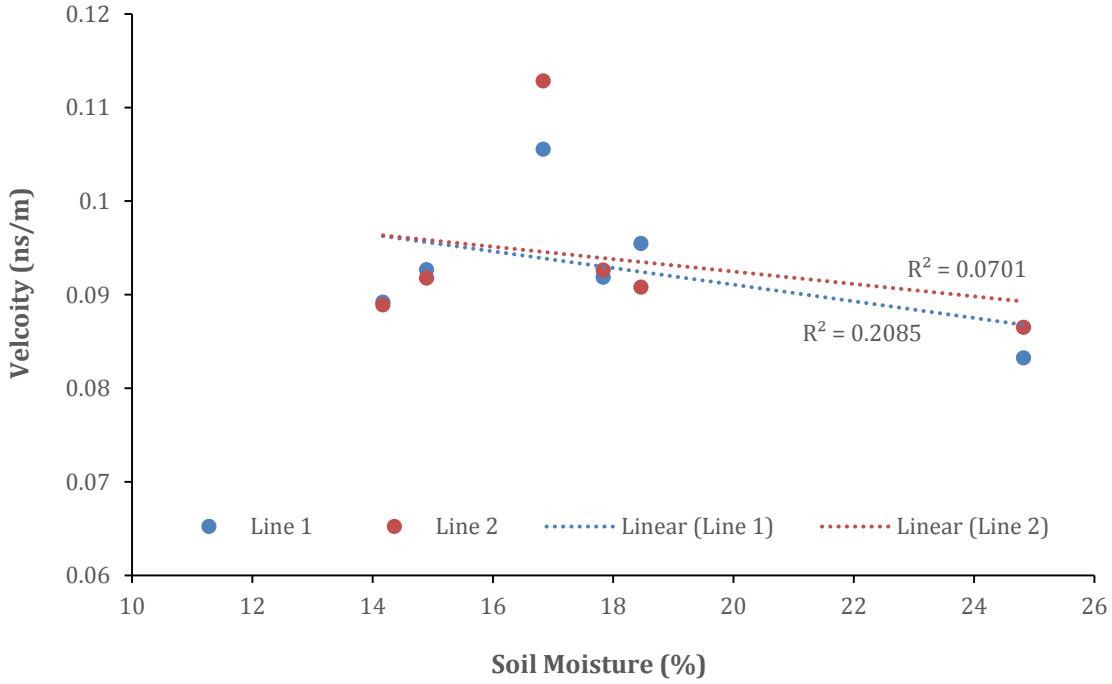

Figure 30. Scatter plot of soil moisture at depth (auger data) and velocity for each CMP line from the turfgrass moisture plot. A linear regression for each determines R^2 value.

III. D'Olive Creek Case Study

The results at the D'Olive Creek study site include one sample from auguring at the surface, 2 CMP lines and (attempted) continuous GPR data. Due to weather and time constraints only one set of data was taken at the study site in December. Although one data set is not sufficient to track moisture trends in CMP data, these data helped us determine the best approach for collecting data in a built floodplain as baseline data for future work. The widest, flattest floodplain bank was chosen for the surveys but due to a recent previous flooding event, debris prevented even acquisition of GPR data. In addition, an auger sample (~4 cm) and was taken but due to inconsistent sample size, it was unusable. The floodplain sediments were very hard and we were unable to collect a full sample. POGO meter measurements confirm that the sediment was extremely dry, also a leading cause as to why the auger measurement was so difficult to acquire (Table 11).

The 2D GPR data did not produce any returns and were abandoned due to inconsistencies with acquisition as a result of flood debris. Our intention was to utilize the 2D continuous profile to locate built floodplain structures, but as a result of the placement of the grid within the floodplain, anything less than 10 m away from the stream channel was not within the survey. Since built floodplain structures are used to stabilize the stream channel, most structures would be within meters of the channels edge.

Velocities calculated from line 1 and line 2 could not be plotted due to lack of temporal data (Table 12). Velocities for the two lines fall within the acceptable range and seem to reflect velocities similar to the dry end at the turfgrass plot moisture experiment. Figure 31 depicts velocities determined from the inverse velocity function in ReflexW™ for one of the lines taken

at the D'Olive Creek case study site. The two velocity calculations from line 1 and 2 are consistent with the very dry POGO meter measurements seen in Table 12.

Although these data were limited, the results confirm that dry sediments result in higher velocities. The POGO meter measurements show volumetric moisture present between 2-8 %, the lowest of any measurements taken throughout this study. Because of this I would expect the velocities of the two lines taken to be higher than any of the velocities taken during the turfgrass plot moisture experiment. These data will become a part of the larger data set when monthly GPR, CMP and auger samples are taken over time to confirm the long-term validity of this monitoring method.

Table 11. POGO meter measurements from the GPR survey at the D'Olive Creek study site. Locations were positioned within the 10 m x 10 m grid. (C= center, E= east, W= west)

Date	Location	Sample #	Moisture %	Temp ˚C	Temp ˚F	Moisture Average	Temp ˚C Average
12/3/2018	C	1	2.30	30.40	86.80	3.10	30.40
12/3/2018	C	2	5.60	30.40	86.80		
12/3/2018	C	3	1.40	30.40	86.80		
12/3/2018	E	4	7.80	30.10	86.20	7.53	30.00
12/3/2018	E	5	7.30	30.10	86.20		
12/3/2018	E	6	7.50	29.80	85.60		
12/3/2018	W	7	3.80	29.80	85.60	2.83	29.60
12/3/2018	W	8	2.10	29.80	85.60		
12/3/2018	W	9	2.60	29.20	84.60		

Table 12. Velocities calculated from the only visit to the D'Olive Creek study site. Due to lack of temporal data plotted trends could not be completed.

Date	Line (1 or 2)	Velocity (m/ns)	Time (ns)	Depth (x)	1/2 depth (1/2x)
12/3/2017	1	0.1599	10	1.599	0.7995
12/3/2017	2	0.10166667	10.5	1.0675	0.53375

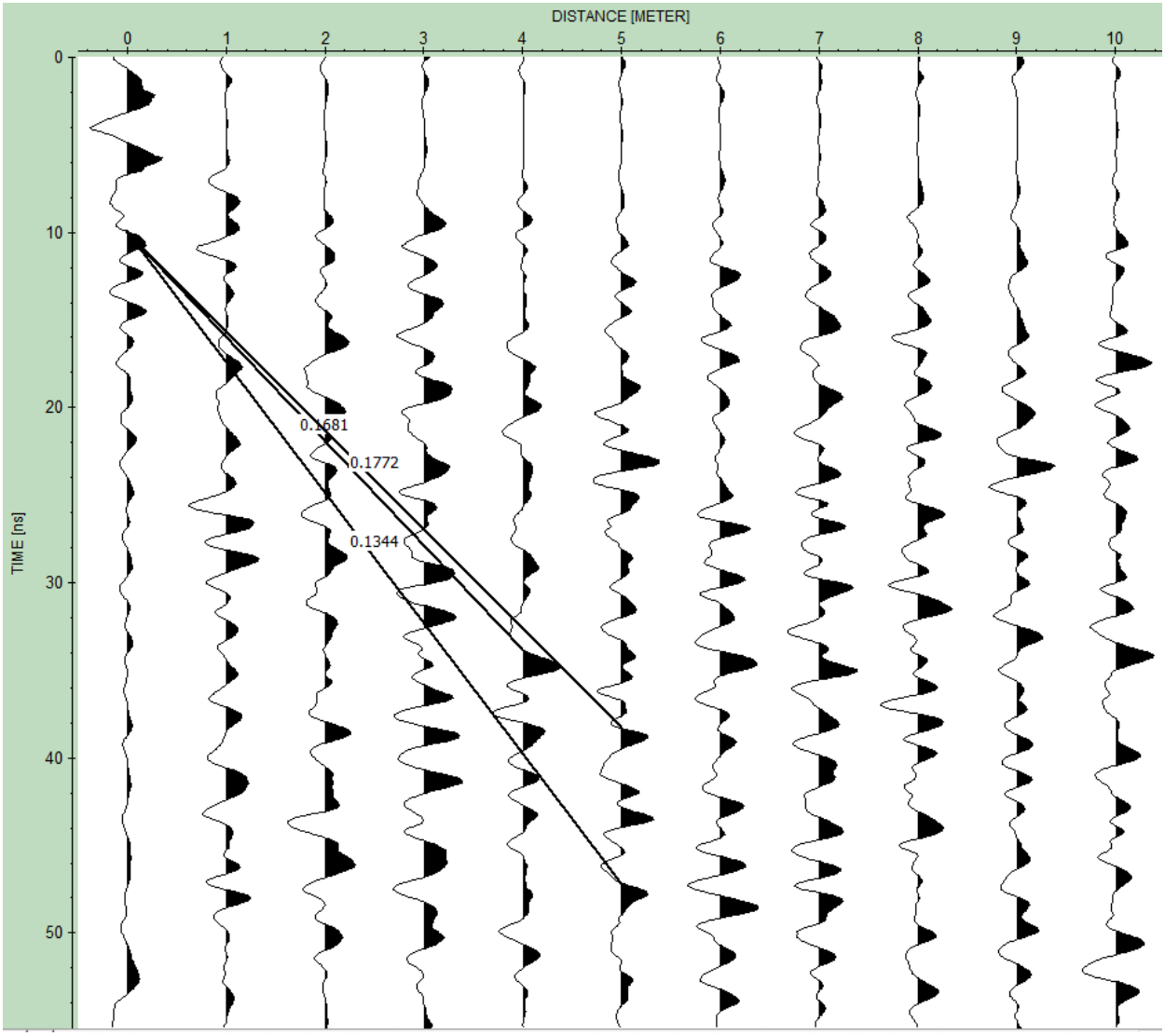

Figure 31. CMP data processed with band-pass and energy-decay filters for CMP line 1 taken on December 3rd, 2017. Black lines are fitted lines for velocity analysis within ReflexW™. Numbers next to lines are individual velocities.

CONCLUSION

This study investigated the potential of using GPR as a long-term monitoring tool on remediated floodplains. GPR experiments including buried objects and testing the detection of subsurface moisture content were collected data across Alabama. These tests confirm that continuous GPR surveys are viable in coastal sediments that have excellent drainage, like those seen at the turfgrass plot, and shallow subsurface areas with distinct clay and fluvial deposits seen at the EV Smith Research Center. CMP data from GPR surveys were found to be consistent with moisture content measurements taken from an auger hole and a POGO meter. CMP data taken at the turfgrass plot and at the D'Olive study site suggest that using CMP GPR surveys as a proxy to estimate subsurface moisture content is possible, but requires calibration for each site.

Metal rebar buried in the subsurface are detectable at shallow depths (<2 m) using both 400 MHz and 900 MHz antennas. The GPR was also able to resolve the trench boundary between disturbed and undisturbed sediments. No other confirmed objects were detectable with the GPR but this is most likely due to experiment flaws including spacing of the objects too closely together.. Some less pronounced hyperbolas in each profile could indicate other materials but more testing is needed to confirm this possibility.

We were able to successfully demonstrate that CMP GPR data used to estimate moisture content can be achieved in coastal sediments in a controlled setting. The velocity of both CMP line 1 and 2 increased as the surface and subsurface dried, as confirmed by auger hole and POGO meter measurements. It does appear that small amounts of rainfall (< 1 inch) may have an effect on surface measurements but it does not affect the subsurface at all. While

the POGO meter measurements do not appear to corroborate a rainfall event, auger hole measurements and CMP data both detect an increase in moisture.

The results from the buried objects and moisture experiments were applied to the study site in the D'Olive Creek watershed. Auger hole measurements were abandoned due to error but the POGO meter confirms that the floodplain had the driest conditions from all three experiments. This resulted in the fastest velocity recorded using the CMP method and confirms the results found during the turfgrass plot moisture experiment. Since CMP is does not require continuous movement of an antenna over the surface of the ground, the problems associated with taking the 2D continuous data did not hinder the CMP results. The results at the D'Olive Creek study site are ongoing and continuous rigorous testing is needed to draw conclusions on the application of GPR to remediated floodplains.

Future Recommendations

Moving forward with validating ground penetrating radar for long-term monitoring requires adjustments as well as revision to existing methods suggested in this thesis. After creating and executing these methodologies, the gaps in understanding have become apparent and should be resolved before the next round of experiments begin. Some limitations that exist for the buried objects GPR survey include being able to distinctly determine the difference between chosen materials on a survey. To do this, creating multiple trenches may be helpful in running isolated experiments to determine the visual identification of specific returns.

Limitations for the moisture plot experiment include being able to isolate all control variables including lateral moisture transfer, existing microbiology and rainfall. While these

conditions do exist in case study examples, quantifying them would help us understand how CMP GPR data attenuates based on the presence of these variables. Determining the correct step increment of antennas for CMP experiments helps to assess the needed resolution of raw data. This is important to any future work to assure that slight changes in moisture will be detected. This can also help in post-processing techniques by making it easier to identify the initial ground wave for velocity analysis. To improve upon velocity analysis, material with a high RDP (i.e., rebar) should also be buried to be able to determine velocity from the known ground wave and determine an exact depth from CMP data.

Other geophysical methods may improve estimates of moisture content. These methods include seismicity, time domain reflectometry (TDR) and electrical resistivity. Additional data may help confirm GPR data or round out a suite of tools used in tandem to monitor floodplains. I believe that the experiments in this thesis are beholden to more rigorous testing if continued support is advised.

REFERENCES

BenDor, T., Lester, T.W., Livengood, A., Davis, A., and Yonavjak, L., 2015, Estimating the Size and Impact of the Ecological Restoration Economy: Plos One, v. 10, doi:10.1371/journal.pone.0128339.

Bernhardt, E.S., and Palmer, M.A., 2007, Restoring streams in an urbanizing world: Freshwater Biology, v. 52, p. 738–751, doi: 10.1111/j.1365-2427.2006.01718.x.

Bigman, D., 2018, GPR Basics: A handbook for ground penetrating radar users: Suwanee, GA, Bigman Geophysical LLC.

Bilskie, J., 2001, Soil water status: content and potential: Campbell Scientific, Inc.

Botha, G.A., Bristow, C.S., Porat, N., Duller, G., Armitage, S.J., Roberts, H.M., Clarke, B.M., Kota, M.W., and Schoeman, P., 2003, Evidence for dune reactivation from GPR profiles on the Maputaland coastal plain, South Africa: Geological Society, London, Special Publications,v. 211, p. 29–46, doi: 10.1144/gsl.sp.2001.211.01.03.

Brantley and Knappenberger, 2016, Upublished whitepaper for D'Olive Creek watershed Stakeholder produced at Auburn University, 4 p.

Bristow, C.S., and Jol, H.M., 2003, An introduction to ground penetrating radar (GPR) in sediments: Geological Society, London, Special Publications, v. 211, p. 1–7, doi:10.1144/gsl.sp.2001.211.01.01.

Carrick, E., 2017, Ground penetrating radar: theory and practice: Oxford, Butterworth-Heinemann.

Coffee, G.L., 2010, Watershed management plan: D'Olive Creek, Tiawasee Creek, and Joe's Branch watersheds, August 2010: Thompson Engineering, Inc. Open- File Report 09-2115-0071, 99p.

Cook, M. R., Assessment of Lake Forest Lake Sediment Trapping Efficiency and Capacity, 2008, Groundwater Assessment Program, Geological Survey of Alabama.

Cook, M.R., Moss, N.E., Rogers, A., and McKinney, M., 2014, Phase II post-restoration analysis of discharge and sediment transport rates in tributaries of Joes Branch in Spanish Fort, Baldwin county, Alabama: Geological Survey of Alabama Open-File Report 1408, 33 p.

Davis, R.A, 2010, Geologic History of Sea Level Change in the Gulf of Mexico: Texas A&M University, http://gulfsealevel.org/Davis,%20Richard.pdf (Accessed March 31st).

Ellis, J.T., Spruce, J.P., Swann, R.A., Smoot, J.C., and Hilbert, K.W., 2010, An assessment of coastal land- use and land-cover change from 1974–2008 in the vicinity of Mobile Bay, Alabama: Journal of Coastal Conservation, v. 15, p. 139–149, doi: 10.1007/s11852-010-0127-y.

Forte, E., and Pipan, M., 2017, Review of multi-offset GPR applications: Data acquisition, processing and analysis: Signal Processing, v. 132, p. 210–220, doi:10.1016/j.sigpro.2016.04.011.

Grote, K., Hubbard, S., and Rubin, Y., 2002, GPR monitoring of volumetric water content in soils applied to highway construction and maintenance: The Leading Edge, v. 21, p. 482–504, doi:10.1190/1.1481259.

Grote, K., Hubbard, S., and Rubin, Y., 2003, Field-scale estimation of volumetric water content using ground penetrating radar ground wave techniques: Water Resources Research, v. 39, doi: 10.1029/2003wr002045.

Grote, K., 2013, A summary of ground penetrating radar techniques for soil water content monitoring: FastTimes, p. 18–29.

GSSI, 2015, Ground Penetrating Radar Data Acquisition Unit SIR-4000: https://www.geophysical.com/products/sir-4000 (accessed February 2018).

Havholm, K.G., Bergstrom, N.D., Jol, H.M., and Running, G.L., 2003, GPR survey of a Holocene aeolian/fluvial/lacustrine succession, Lauder Sandhills, Manitoba, Canada: Geological Society, London, Special Publications, v. 211, p. 47–54, doi: 10.1144/gsl.sp.2001.211.01.04.

Hubbard, S., Lunt, I., Grote, K., and Rubin, Y., 2003, Vineyard soil water content: mapping small scale variability using ground penetrating radar: Geoscience Canada Reprint, v. 9, p.193-202.

Huisman, J., Sperl, C., Bouten, W., and Verstraten, J., 2001, Soil water content measurements at different scales: accuracy of time domain reflectometry and ground-penetrating radar: Journal of Hydrology, v. 245, p. 48–58, doi: 10.1016/s0022-1694(01)00336-5.

Huisman, J.A., Hubbard, S.S., Redman, J.D., and Annan, A.P., 2003, Measuring Soil Water Content with Ground Penetrating Radar: A Review: Vadose Zone Journal, v. 2, p. 476–91, doi: 10.2113/2.4.476.

Johnson, B.L., Richardson, W.B., and Naimo, T.J., 1995, Past, Present, and Future Concepts in Large River Ecology: BioScience, v. 45, p. 134–141, doi: 10.2307/1312552.

Jol, H.M., 2009, Ground Penetrating Radar: Theory and Applications: Amsterdam, Elsevier Science, 524p.

Jol, H.M., Smith, D.G., and Meyers, R.A., 1995, Digital Ground Penetrating Radar (GPR): A New Geophysical Tool for Coastal Barrier Research (Examples from the Atlantic, Gulf and Pacific Coasts, U.S.A.): Journal of Coastal Research, v. 12, no. 4, p. 960-968.

Khakiev, Z., Shapovalov, V., Kruglikov, A., Morozov, A., and Yavna, V., 2014, Investigation of long term moisture changes in trackbeds using GPR: Journal of Applied Geophysics, v. 110, p. 1–4, doi: 10.1016/j.jappgeo.2014.08.014.

Lambin, E.F., Turner, B.L., Geist, H.J., and Agbola, S.B., 2001, The causes of land-use and land-cover change: moving beyond the myths. Global Environmental Chang, v. 11, p. 261-269.

Lunt, I., Hubbard, S., and Rubin, Y., 2005, Soil moisture content estimation using ground-penetrating radar reflection data: Journal of Hydrology, v. 307, p. 254–269, doi: 10.1016/j.jhydrol.2004.10.014.

McMillan, S.K., and Noe, G.B., 2017, Increasing floodplain connectivity through urban stream restoration increases nutrient and sediment retention: Ecological Engineering, v. 108, p. 284–295, doi: 10.1016/j.ecoleng.2017.08.006

Merz, B., and Plate, E.J., 1997, An analysis of the effects of spatial variability of soil and soil moisture on runoff: Water Resources Research, v. 33, p. 2909–2922, doi: 10.1029/97wr02204.

O'Neal, M.L., and Dunn, R.K., 2003, GPR investigation of multiple stage-5 sea-level fluctuations on a siliciclastic estuarine shoreline, Delaware Bay, southern New Jersey, USA:Geological Society, London, Special Publications, v. 211, p. 67–77, doi:10.1144/gsl.sp.2001.211.01.06.

Orchard, V.A., and Cook, F., 1983, Relationship between soil respiration and soil moisture: Soil Biology and Biochemistry, v. 15, p. 447–453, doi: 10.1016/0038-0717(83)90010-x.

Overmeeren, R.V., Sariowan, S., and Gehrels, J., 1997, Ground penetrating radar for determining volumetric soil water content; results of comparative measurements at two test sites: Journal of Hydrology, v. 197, p. 316–338, doi: 10.1016/s0022-1694(96)03244-1.

Reed, P.C., 1971, Geology of Baldwin County, Alabama: Geologic Society of Alabama Special Map 94, 9p.

Salisbury, M., 2018, Analysis of the D'Olive Creek Watershed: Identifying the Local Drivers That Have led to Stream Degradation and how they compare to the Drivers of the Fly Creek Watershed [M.S. thesis]: Auburn University, *Unpublished*.

Smith, W.E, 1988, Geomorphology of the Mobile Delta: Geological Survey of Alabama, Bulletin 132, 117p.

Steelman, C.M., and Endres, A.L., 2012, Assessing vertical soil moisture dynamics using multi-frequency GPR common-midpoint soundings: Journal of Hydrology, v. 436-437, p. 51–66, doi: 10.1016/j.jhydrol.2012.02.041.

Steelman, C.M., Endres, A.L., and Jones, J.P., 2012, High-resolution ground-penetrating radar monitoring of soil moisture dynamics: Field results, interpretation, and comparison with unsaturated flow model: Water Resources Research, v. 48, doi: 10.1029/2011wr011414.

USDA NRSC, 2017, Web Soil Survey: https://websoilsurvey.sc.egov.usda.gov/App/WebSoilSurvey.aspx (accessed March 2017)

Van Dam, R.L., Van den Berg, E., Schaap, M.G., Broekema, L.H., and Schlager, W., 2003, Radar reflections from sedimentary structures in the vadose zone: Geological Society, London, Special Publications, v. 211, p. 257–273, doi: 10.1144/gsl.sp.2001.211.01.21.

Violin, C.R., Cada, P., Sudduth, E.B., Hassett, B.A., Penrose, D.L., and Bernhardt, E.S., 2011, Effects of urbanization and urban stream restoration on the physical and biological structure of stream ecosystems: Ecological Applications, v. 21, p. 1932–1949, doi: 10.1890/10-1551.1.

Vittor, B.A., Wetland condition evaluation: D'Olive Creek, Tiawasee Creek, and Joe's Branch watersheds (Baldwin County, Alabama), 2010: Thompson Engineering, Mobile, Alabama.

APPENDIX A: Photo Documentation

Date	Study Site	Description	Number
9/27/2017	BO	Rebar and rock/concrete used in trench with scale	1
9/27/2017	BO	One blue 6 L carboy and one plastic cooler used in trench with scale	2
9/27/2017	BO	Six logs used in both layers of buried objects with ruler for scale	3
9/27/2017	BO	First layer of objects with a Sam for scale	4
9/27/2017	BO	Filling trench in partially to put second layer of object on top of	5
9/27/2017	BO	Second layer of objects	6
9/27/2017	BO	Filled and covered trench with a Mike for scale	7
10/1/2017	BO	Trench surface after settling and Sam taking auger sample	8
10/1/2017	BO	Marking out 0.3 m spacing for GPR survey	9
10/3/2017	MO	Using 400 MHZ antenna for 2D profile with survey wheel	10
10/3/2017	MO	Two antennas (400 & 900 MHz) and control unit to complete CMP survey	11
12/3/2017	DO	Oblique view of floodplain used to complete GPR survey at study site, yellow shape indicates floodplain survey was taken on	12


1
2017.09.27 12:02


2
WATER


3


4


5
JCB


6


7

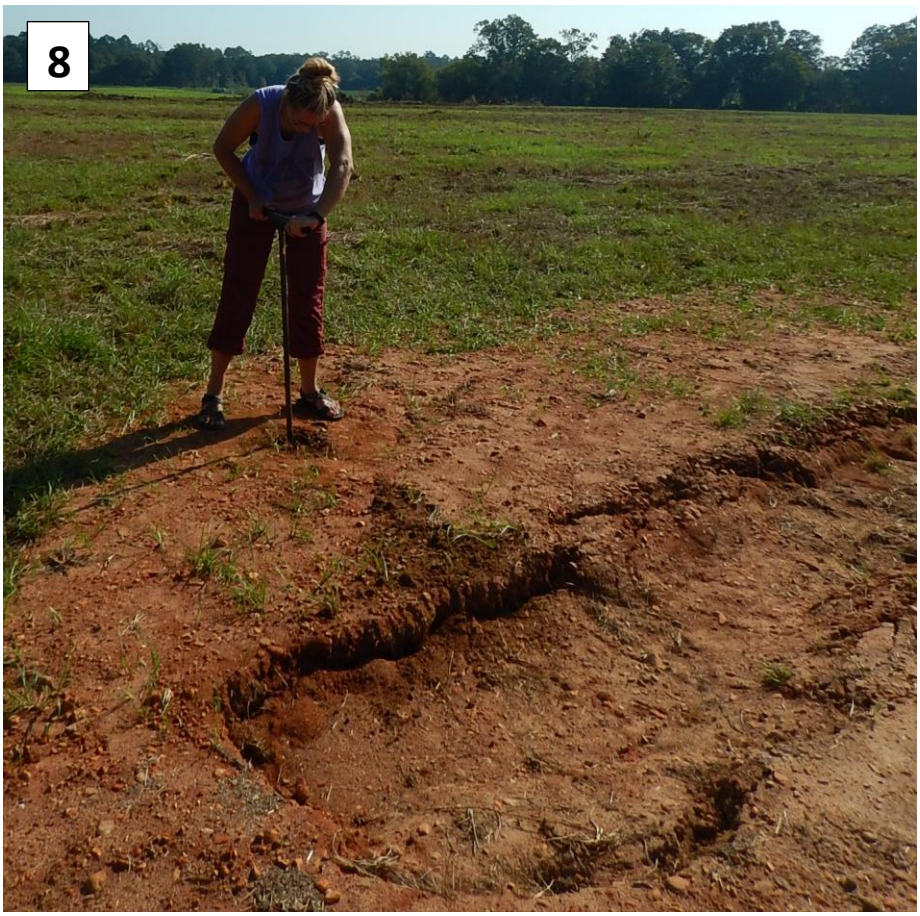
8


9
2017 10 01 10 42


10
2017.11.03 10:07

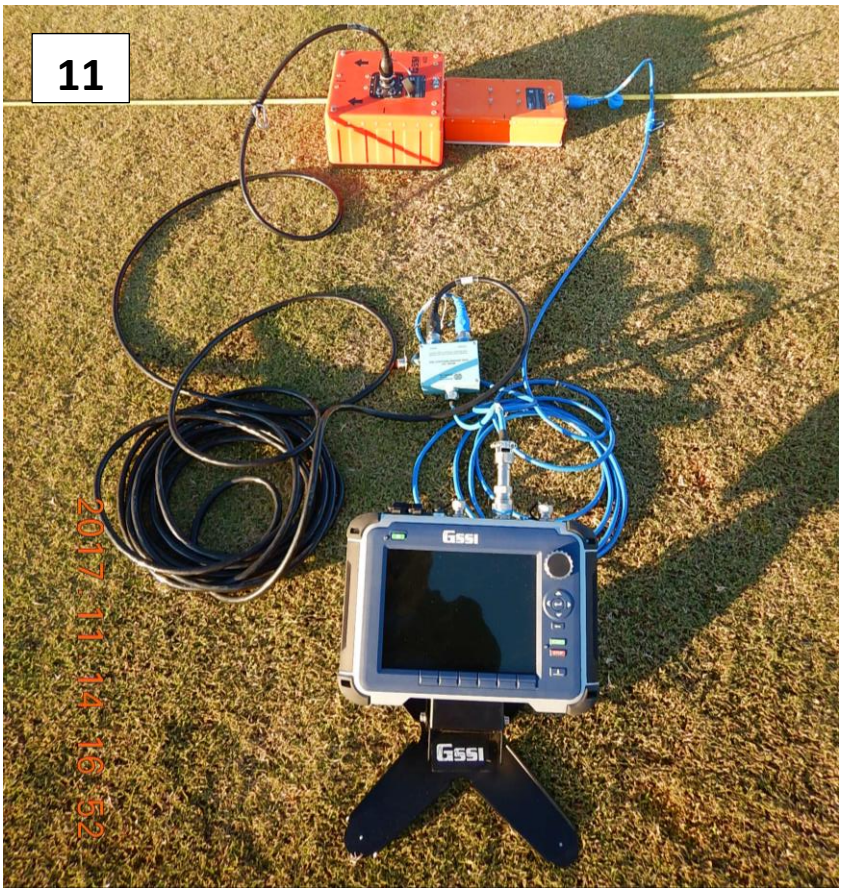
11
GSSI
GSSI
2017.11.14 16:52


12

APPENDIX B: Supplementary Data

Table A. Summary of POGO meter measurements taken from the buried objects experiment at EV Smith research center after GPR surveys were completed. The POGO meter is intended for surface measurements and was used in DH measurements, which may indicate inaccurate moisture measurements. (DH= down hole depth, surface=within 7 cm of the surface)

Date	Location	Sample #	Moisture %	Temp ˚C	Temp ˚F	Moisture Average	Temp ˚C Average
10/13/2017	Surface	1	12.00	26.40	79.50		
10/13/2017	Surface	2	13.20	27.20	81.00		
10/13/2017	Surface	3	19.40	27.20	81.00		
10/13/2017	Surface	4	15.70	27.50	81.50	15.08	27.08
10/13/2017	0.5 m DH	5	3.50	28.90	84.00		
10/13/2017	0.5 m DH	6	4.70	28.60	83.50		
10/13/2017	0.5 m DH	7	3.90	28.60	83.50	4.03	28.70
10/13/2017	DH pit hole	8	18.90	37.40	83.50		
10/13/2017	DH pit hole	9	18.80	36.50	99.30		
10/13/2017	DH pit hole	10	18.20	35.70	96.30	18.63	93.03